

NASA
CR
3121
c.1

NASA Contractor Report 3121

LOAN COPY RETURN
AFWL TECHNICAL LIBRARY
KIRTLAND AFB NM
SOL 900

TECH LIBRARY KAFB, NM


Incorporation of Coupled Nonequilibrium Chemistry Into a Two-Dimensional Nozzle Code (SEAGULL)

Alan W. Ratliff

CONTRACT NAS1-14754
APRIL 1979

NASA





0061905

NASA Contractor Report 3121

Incorporation of Coupled Nonequilibrium Chemistry Into a Two-Dimensional Nozzle Code (SEAGULL)

Alan W. Ratliff

*Lockheed Missiles & Space Company, Inc.
Huntsville, Alabama*

Prepared for
Langley Research Center
under Contract NAS1-14754



National Aeronautics
and Space Administration

**Scientific and Technical
Information Office**

1979

CONTENTS

<u>Section</u>		<u>Page</u>
	SUMMARY AND INTRODUCTION	v
1	SYMBOLS	1
2	DISCUSSION	3
2.1	Baseline Nozzle Code - Program SEAGULL	3
2.2	Modified Nozzle Code	3
2.3	Development of Equations	3
2.4	Solution Technique	6
2.5	Boundary Conditions	13
2.6	Shock Waves	14
2.7	Contact Surfaces	21
2.8	Thermodynamic Properties	21
2.9	Vibrational Nonequilibrium	22
Appendixes		
A	Shock Fitting Method for Complicated Two-Dimensional Supersonic Flows	23
B	Input Guide and Sample Cases	31
	REFERENCES	51

SUMMARY AND INTRODUCTION

During the past decade several excellent computer codes for analyses of complicated flow fields have been developed. NASA-Langley's SEAGULL program (Appendix A) that treats multiple shock waves and contact surfaces, using a floating shock fitting technique, is one such code. Previously, calculations performed with this code were limited to the ideal gas assumption. It is the purpose of this document to describe the extension of the code to handle real gas effects via the incorporation of a general finite rate chemistry and vibrational energy exchange package.

This document and the associated computer code (modified SEAGULL) now provide NASA-Langley with a benchmark finite rate general chemistry nozzle and plume code. The modified code retains all of its original features plus the capability to treat chemical and vibrational nonequilibrium chemistry. The chemistry package is extremely general in nature, handling any chemical reaction or vibrational energy exchange mechanism as long as thermodynamic data and rate constants are available for all participating species.

1. SYMBOLS

<u>Symbol</u>	<u>Description</u>
A	defined as used
b(z)	lower duct wall ordinate
c(z)	upper duct wall ordinate
C _p	specific heat at constant pressure
C _v	specific heat at constant volume
f(s)	entropy production (Eq. 4)
f _i	weighting factors (Eq. 15)
F _i	species mole/mass ratio
G	defined by Eq. (50)
h	static enthalpy
H	total enthalpy
k	reaction rate constant
K _p	equilibrium constant
P	natural log of pressure
p	pressure
q	total velocity
r	radial coordinate
R	universal gas constant
R	universal gas constant divided by global molecular weight

<u>Symbol</u>	<u>Description</u>
s	entropy
T	temperature
u	radial velocity component
w	axial velocity component
\dot{w}_i	net production rate of species i
X	transformed radial coordinate
y	axial coordinate
z	axial coordinate

Greek

α_i	species mole fraction
β	defined by Eq. (3)
γ	ratio of specific heats
$\nu_i^!, \nu_i^{!!}$	stoichiometric coefficients
ρ	density
ψ_i	species molecular weight
ψ	global molecular weight

Subscripts

i	refers to species i
in.	refers to initial conditions

2. DISCUSSION

2.1 BASELINE NOZZLE CODE - PROGRAM SEAGULL

Program SEAGULL is a computer code for the numerical analysis of complex two-dimensional or axisymmetric supersonic inviscid flows of a perfect gas. The fundamental limitation of this program is that the component of the Mach number in the axial direction at any point in the flow field must remain supersonic. The program was primarily designed for the analysis of internal flows. It can compute the flow field produced by a single duct or several ducts that are merged. Although designed for internal flows, it can also compute jets and plumes. The program continuously monitors the flow field to detect the formation of shock waves. All discontinuities are treated explicitly, and all interactions are treated by a locally exact solution. A description of the method used is given in Appendix A.

2.2 MODIFIED NOZZLE CODE

The modified program Seagull is now a computer code for the numerical analysis of complex two-dimensional or axisymmetric supersonic inviscid flows with fully coupled nonequilibrium chemistry. The code retains all the salient features discussed in Section 2.1, plus the additional capability to treat frozen or finite rate chemically reacting flows. The generalized chemistry package included in the modified Seagull also permits the analysis of vibrational nonequilibrium energy exchanges.

2.3 DEVELOPMENT OF EQUATIONS

The basic equations governing the flow of gases with nonequilibrium reacting chemistry are the following:

$$\nabla \cdot \rho \bar{q} = 0 \quad \text{Global Continuity}$$

$$\nabla \bar{q} \cdot \rho \bar{q} + \nabla p = 0 \quad \text{Momentum}$$

$$\rho \bar{q} \cdot \nabla H = 0 \quad \text{Energy}$$

$$\rho \bar{q} \cdot \nabla F_i - \dot{w}_i = 0 \quad \text{Species Continuity}$$

$$p = \rho \gamma T \sum_{i=1}^N \frac{\alpha_i}{\psi_i} \quad \text{Equation of State}$$

$$H = h + \frac{1}{2} \nabla (\bar{q} \cdot \bar{q}) \quad \text{Total Enthalpy}$$

$$\dot{w}_i = \frac{\rho}{\psi_i} \sum_{j=1}^M (\nu_{i,j}'' - \nu_{i,j}') \left[k_f \prod_{\ell=1}^N F_{\ell}^{\nu_{\ell}', j} - k_b \prod_{\ell=1}^N F_{\ell}^{\nu_{\ell}'', j} \right]$$

General Species
Production Rate

where N species are involved in M reactions.

These equations are expanded in a Cartesian coordinate system, scaled (i.e., nondimensionalized) with respect to some initial reference conditions, and are then solved in the modified SEAGULL code.

To avoid unnecessarily complicating the discussion, the remainder of the derivation is shown for a two-dimensional case only. The code, however, can also handle axisymmetries flows.

Scaled and expanded, the equations then become

$$\left. \begin{aligned} \beta P_z + w u_r + A_1 w u P_r - uw_r - \frac{w}{A_2} f(s) &= 0 \\ \beta w_z + \frac{T}{\psi} u_r + A_1 w u w_r - A_1 \frac{T}{\psi} u P_r + \frac{T}{A_2 \psi} f(s) &= 0 \\ u_z + \frac{u}{w} u_r + \frac{T}{w \psi} P_r &= 0 \\ w F_{i_z} + u F_{i_r} - \frac{\dot{w}}{\rho} &= 0 \\ H_z + \frac{u}{w} H_r &= 0 \end{aligned} \right\} \quad (2)$$

where the subscripts refer to differentiation with respect to the r, z coordinates.

β, A_1 and A_2 are conveniently defined as follows:

$$\left. \begin{aligned} \beta &= A_1 w^2 - \frac{T}{\psi} \\ A_1 &= 1 - \frac{\gamma_{in} - 1}{A_2} \\ A_2 &= \gamma_{in} C_p \end{aligned} \right\} \quad (3)$$

The function $f(s)$ is the entropy production due to finite rate chemical reactions.

$$f(s) = (\bar{q} \cdot \nabla s)_{chem} \quad (4)$$

The general set of governing equations (Eq. (2)) are then recast in terms of the computational coordinates (X, Z) that are defined by

$$X = (r - b(z))/(c(z) - b(z)) \quad (5)$$

and

$$Z = z$$

where $b(z)$ and $c(z)$ define the lower and upper walls of the duct or nozzle.

All the primary variables in the equation set are scaled with respect to the initial conditions. The pressure, density, temperature and molecular weight are non-dimensionalized by p_{in} , ρ_{in} , T_{in} , ψ_{in} , respectively. Velocity is conveniently scaled by $\sqrt{p_{in}/\rho_{in}}$ and entropy is non-dimensionalized by the specific heat at constant volume $C_{v_{in}}$, i.e., $S = ([S] - [S_{in}])/C_{v_{in}}$.

The specific heat at constant pressure, C_p , is scaled with respect to its initial value, $[C_p] = [C_p]/[C_{p_{in}}]$. Static enthalpy is non-dimensionalized by $C_{p_{in}} T_{in}$, and for consistency the total enthalpy equation then becomes

$$H_T = h + \frac{[\mathcal{R}]}{[C_{p_{in}}]} (u^2 + w^2) \psi \quad (6)$$

where all values are non-dimensional except $[\mathcal{R}]$ and $[C_{p_{in}}]$.

The finite rate chemistry parameters, of course, have dimensional characteristics. Interrelationships between the flow field and the finite rate reactions are treated internally by temporarily dimensioning the variables appearing in the species continuity equations. The reacting chemistry calculation is then carried out and the results are subsequently non-dimensionalized.

2.4 SOLUTION TECHNIQUE

A finite difference numerical scheme utilizing the explicit MacCormack operator is used to integrate the equations for conservation of global mass, momentum and energy. The species conservation equations are solved by an implicit technique similar to that developed by Moretti (Ref. 1). This method was chosen to provide good stability characteristics in the overall numerical scheme.

The general solution technique is discussed adequately in Appendix A. The same methodology is retained in the modified SEAGULL with the finite rate reacting chemistry. The only exception is the species continuity equation set which is solved by the following technique.

A detailed description of the rate processes that occur in finite rate reacting flows requires that a myriad of mechanisms be considered to include all the possible chemical and vibrational reactions of dissociation, formation, recombination, etc.

All of these, however, can be treated with a very general formalism. In the form usually quoted in chemical kinetics (Ref. 2) the phenomenological law of mass action states that the rate of a reaction is proportional to the product of the concentrations of the reactants. Thus, for a general reaction of the form

$$\sum_{j=1}^N \nu_j^! A_j = \sum_{j=1}^N \nu_j'' A_j \quad (7)$$

the net rate of production \dot{w}_i for any participating species for which the stoichiometric coefficients $\nu_i^!$ and ν_i'' are not equal can then be written as

$$\dot{w}_i = \frac{\rho}{\psi_i} \sum_{j=1}^M (\nu_i'', j - \nu_i^!, j) \left[k_f \prod_{\ell=1}^N F_\ell^{\nu_\ell^!, j} k_b \prod_{\ell=1}^N F_\ell^{\nu_\ell'', j} \right] \quad (8)$$

Assuming small deviations from equilibrium, the forward and backward reaction rate constants, k_f and k_b , respectively, can be related to the concentration equilibrium constant and to the pressure equilibrium constant as follows:

$$\frac{k_f}{k_b} = K_c = K_p (\mathfrak{R} T)^{\sum_{i=1}^N (\nu_i^! - \nu_i'')} \quad (9)$$

The significance of the pressure equilibrium constant K_p is that it can be easily evaluated for any reaction using tabulated values of K_f the equilibrium constant for formation from the elements. Values of K_f are commonly tabulated in conjunction with specific heats, entropies and enthalpies as a function of temperature, and are available in general for most species. An equally

convenient method exists for determining K_p from the change of free energy accompanying the reaction, i.e.,

$$K_p = \exp(-\Delta G/RT) \quad (10)$$

where ΔG is the change in free energy during the reaction process. Free energy values are also available for most species in tabular form. This method is used to compute K_p in Program SEAGULL. The JANNAF thermochemical tables (Ref.4) are used as the source for obtaining input data for various chemical systems. ΔG is computed directly by taking the difference in free energy between the products and reactants.

For reasons of computational speed and efficiency, the program contains explicit expressions, as obtained from Eq.(11), for the most commonly encountered reaction mechanisms. Twelve types of reaction mechanisms are considered as possible contributors to the calculation of the net rate of production, \dot{w}_i .

Reaction Type

(1, 7)	A + B		C + D
(2, 8)	A + B + M		C + M
(3, 9)	A + B		C + D + E
(4, 10)	A + B		C
(5, 11)	A + M		C + D + M
(6, 12)	A + M		C + M

Reaction types (7) through (12) correspond to reaction types (1) through (6), but proceed in the forward direction only.

To reduce roundoff and truncation errors, the forward and backward rates for each reaction are computed separately. All contributions to the molar rate of production of a given species are then computed and added algebraically to form matrix coefficients (discussed later). Since reaction types (7) through (14) proceed in the forward direction only, the second term on the right-hand side of Eq. (11) is disregarded in calculating the contributions to the coefficient matrix.

In reactions (2), (5) and (6) as well as in (8), (11) and (12), M denotes a third body species which can be specified. For these reactions the situation often occurs where for various third bodies the respective rate constants differ only by a constant multiplier. These multipliers can be considered as third body efficiencies or weighting factors. If such a case is encountered, the third body species mole mass ratio F_M becomes effectively a fictitious mole mass ratio, consisting of the weighted sum over all those species having a nonzero weighting factor, i.e.,

$$F_M = \sum_i f_i F_{M_i} \quad (12)$$

where f_i are the weighting factors.

The forward rate constant, k_f , is generally a function of temperature. It is most often expressed in Arrhenius form. Again, for speed and efficiency in computation, the rate constants are divided into five types:

Rate Constant Type

(1)	$k_f = A$	
(2)	$k_f = AT^{-N}$	
(3)	$k_f = A \exp(B/\mathcal{R}T)$	(13)
(4)	$k_f = AT^{-N} \exp(B/\mathcal{R}T)$	
(5)	$k_f = AT^{-N} \exp(B/\mathcal{R}T^M)$	

The equations presented in this document provide a very general formalism for the evaluation of various rate processes. The specification of particular systems and associated rate constant will be up to the program user.

Consider now the general species continuity equation

$$\rho \bar{q} \cdot \nabla F_i = \dot{w}_i \quad (14)$$

and making use of the foregoing discussion of the rate process we now proceed to describe a calculational technique for determining the individual species composition on a point-by-point basis. The description of this process is substantially simplified if Eq. (11) is specialized to a particular reaction type, say number (7) from Eq. (14) which is a one-way, two-body reaction.



the net production rate for this process is

$$\dot{w} = -k_f \rho^2 F_A F_B \quad (16)$$

and the species continuity equation for species B then becomes

$$\rho \bar{q} \cdot \nabla F_B = -k_f \rho^2 F_A F_B \quad (17)$$

This equation can readily be solved using finite difference techniques employing explicit relationships, such as Euler or more sophisticated schemes, such as Runge-Kutta. The step size for integrating this equation, however, is severely limited by stability criteria. It can be seen from Eq. (20) that the rate of change of a species along the streamline becomes increasingly larger as the flow speed is slowed, the density increased, or for fast reaction rates. In rocket engine problems, combinations of slow speeds, high densities and fast reaction rates (i.e., quasi-equilibrium) are quite common and integration step sizes so small (i.e., $< 10^{-8}$ meters) are encountered that the solution becomes impractical in terms of computation time.

For this reason, the technique described in Ref. 3 based on a linearization of the production rates was utilized. Writing Eq. (20) in finite difference form over an integration step from station n at $z = z_o$ to $n+1$ at $z = z_o + \Delta z$

$$F_{B_{n+1}} = F_{B_n} - \frac{k_f \Delta z \rho}{q} F_{A_{n+1}} F_{B_{n+1}} - \frac{u}{w} \Delta z \frac{\partial F_{B_n}}{\partial r_n} \quad (18)$$

And evaluating all the species concentrations at the downstream point results in a set of simultaneous nonlinear algebraic equations. The lateral gradient term $\frac{\partial F_{B_n}}{\partial r_n}$ is evaluated at the upstream station n and uses windward differences.

In order to solve these equations we must then linearize the term $F_{A_{n+1}} F_{B_{n+1}}$ which is accomplished following the lead of Ref. 3. If this term is expanded in terms of its values at station n along with the increments over n to $n+1$ we can obtain the following expression.

$$F_{A_{n+1}} F_{B_{n+1}} = F_{A_n} F_{B_{n+1}} + F_{B_n} F_{A_{n+1}} - F_{A_n} F_{B_n} \quad (19)$$

neglecting products of differentials which are assumed to be of second order importance. Equation (21) can now be written in its linearized form. Let $C = \Delta z k_f \rho / w$, then

$$F_{B_{n+1}} = F_{B_n} - C \left[F_{A_n} F_{B_{n+1}} + F_{B_n} F_{A_{n+1}} - F_{A_n} F_{B_n} \right] - \frac{u}{w} \Delta z \frac{\partial F_{B_n}}{\partial r_n} \quad (20)$$

and similarly,

$$F_{A_{n+1}} = F_{A_n} - C \left[F_{A_{n+1}} F_{B_n} + F_{B_{n+1}} F_{A_n} - F_{A_n} F_{B_n} \right] - \frac{u}{w} \Delta z \frac{\partial F_{A_n}}{\partial r_n}$$

Equation (20) can then be expressed in terms of a set of unknowns and calculable coefficients, C. Rewriting these we obtain

$$\begin{aligned} F_{B_{n+1}} &= Q_{B_n} - C F_{A_n} (F_{B_{n+1}}) - C F_{B_n} (F_{A_{n+1}}) \\ F_{A_{n+1}} &= Q_{A_n} - C F_{B_n} (F_{A_{n+1}}) - C F_{A_n} (F_{B_{n+1}}) \end{aligned} \quad (21)$$

where

$$Q_{i_n} = F_{i_n} + C F_{i_n} F_{j_n} - \frac{u}{w} \Delta z \frac{\partial F_i}{\partial r_n} \quad (22)$$

$$\begin{aligned} F_{A_{n+1}} (1 + C F_{B_n}) + (C F_{A_n}) F_{B_{n+1}} &= Q_{A_n} \\ F_{A_{n+1}} (C F_{B_n}) + (1 + C F_{A_n}) F_{B_{n+1}} &= Q_{B_n} \end{aligned} \quad (23)$$

A matrix can now be formed using totally known information.

$$\begin{bmatrix} 1 + C F_{B_n} & C F_{A_n} \\ C F_{B_n} & 1 + C F_{A_n} \end{bmatrix} \begin{bmatrix} F_{A_{n+1}} \\ F_{B_{n+1}} \end{bmatrix} = \begin{bmatrix} Q_{A_n} \\ Q_{B_n} \end{bmatrix} \quad (24)$$

The matrix $[A] [X] = [B]$ is then solved for the unknown compositions $F_{A_{n+1}}$, $F_{B_{n+1}}$ via a triangulation technique. Although consuming more time per integration step than an explicit formulation, the implicit technique employed here is unconditionally stable permitting much larger step sizes, thus allowing solutions to be obtained for problems where the small steps required by the explicit technique prevented even the consideration of the case. Finally it should be recalled that an extremely simple case was chosen only for purposes of illustration and the general technique coded in the modified Program SEAGULL will handle many species with multiple reactions.

2.5 BOUNDARY CONDITIONS

By combining the two momentum equations we obtain

$$\tau_z + w^2 \frac{\tau A_1}{\beta} \tau_r + \left(\frac{A_1 w^2 \tau^2}{\beta} + 1 \right) \frac{T}{\psi w^2} P_r - \frac{T}{\beta \psi w A_2} f(s) = 0 \quad (25)$$

where $\tau = u/w$.

The global continuity equation is used in the form

$$P_z + \frac{w^2}{\beta} (\tau A_1 P_r + \tau_r) - \frac{w}{A_2 \beta} f(s) = 0. \quad (26)$$

Now, using Eqs. (28) and (29) that involve partials of P and τ only, a characteristics compatibility equation can be written

$$\frac{d\tau}{dz} + \frac{T}{w^2 \psi} \sqrt{\frac{A_1(u^2 + w^2)}{T/\psi}} - 1 \frac{dP}{dz} = \text{RHS} \quad (27)$$

where the right-hand side (RHS) is:

$$\text{RHS} = \frac{f(s)}{A_2} \left[\frac{T}{\beta \psi w} \left(\tau \pm \sqrt{\frac{A_1(u^2 + w^2)}{T/\psi}} - 1 \right) \right] \quad (28)$$

Then by combining these equations with the chain rule definitions,

$$\left. \begin{aligned} \frac{dP}{dz} &= \frac{\partial P}{\partial z} + \lambda \frac{\partial P}{\partial r} \\ \frac{d\tau}{dz} &= \frac{\partial \tau}{\partial z} + \lambda \frac{\partial \tau}{\partial r} \end{aligned} \right\} \quad (29)$$

an equation for the axial pressure variation is obtained in terms of known quantities.

$$P_z = -\lambda P_r \mp \frac{w^2 (\text{RHS} - \tau_z - \lambda \tau_r)}{\frac{T}{\psi} \sqrt{\frac{A_1(u^2 + w^2)}{T/\psi} - 1}} \quad (30)$$

where

$$\lambda = \frac{w^2 \tau A_1}{\beta} \pm \frac{T}{\beta \psi} \sqrt{\frac{A_1(u^2 + w^2)}{T/\psi} - 1} \quad (31)$$

By integrating Eq. (30), the pressure is obtained at the new wall point and the velocity is computed from the streamwise momentum equation

$$\rho q \frac{\partial q}{\partial s} = - \frac{\partial P}{\partial s} \quad (32)$$

Velocity components u and w are then obtained from the known wall slope. The boundary conditions are completed by integrating the species continuity equations along the wall in a manner similar to that used for the interior points.

2.6 SHOCK WAVES

The general scheme outlined in Appendix A is utilized for computing shock wave information. The original ideal gas analysis was supplemented by the addition of methodology to handle reacting gas calculations across the shocks.

Figure 1 illustrates a stream tube passing through an oblique shock wave. This wave, which is extremely thin, will cause an almost instantaneous rise in pressure and temperature. For some distance downstream of the shock wave (in a reacting gas) a non-equilibrium zone will exist followed by a return to chemical equilibrium. The following analysis discusses the fluid flow properties in such a way that the non-equilibrium process need not be specified in order to arrive at an exact solution for the gas properties. It is impossible to determine the location of the new equilibrium shock point location without a detailed description of the non-equilibrium reaction process. It will be assumed therefore that this zone is thin and that no significant errors are introduced by letting the downstream physical location lie on the upstream location.

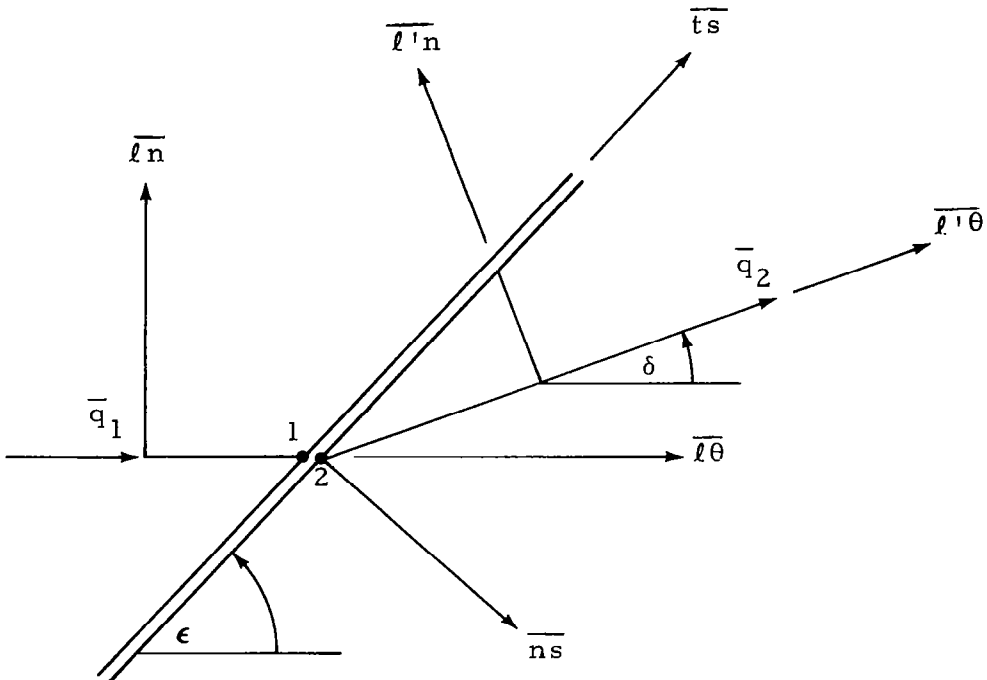
Consider a control surface as shown in the figure. The conservation of mass yields:

$$\rho_2 q_2 A_2 - \rho_1 q_1 A_1 = 0 \quad (33)$$

Let \overline{ns} and \overline{ts} be unit vectors normal and tangent to the shock surface, the unit vectors parallel and perpendicular to the streamline upstream of the shock are

$$\overline{\ell \theta} = \sin \epsilon \overline{ns} + \cos \epsilon \overline{ts}$$

$$\overline{\ell n} = -\cos \epsilon \overline{ns} + \sin \epsilon \overline{ts} \quad (34)$$



and the unit vectors parallel and perpendicular to the streamline downstream of the shock are:

$$\overline{\ell \theta'} = \sin (\epsilon - \delta) \overline{ns} + \cos (\epsilon - \delta) \overline{ts}$$

$$\overline{\ell n'} = -\cos (\epsilon - \delta) \overline{ns} + \sin (\epsilon - \delta) \overline{ts} \quad (35)$$

Conservation of momentum gives

$$-(p_1 + \rho_1 q_1^2) A_1 \frac{\overline{t\theta}}{\tan \epsilon} + \frac{p_1 A_1}{\tan \epsilon} \frac{\overline{tn}}{\overline{t\theta}} + (p_2 + \rho_2 q_2^2) A_2 \frac{\overline{t\theta'}}{\tan(\epsilon - \delta)} - \frac{p_2 A_2 \overline{tn}}{\tan(\epsilon - \delta)} \quad (36)$$

and, after substitution of Eqs. (34) and (35) and setting each component to zero, Eq. (36) becomes,

$$\rho_2 q_2^2 \cos(\epsilon - \delta) A_2 - \rho_1 q_1^2 A_1 \cos \epsilon = 0 \quad (37)$$

$$(p_1 + \rho_1 q_1^2) A_1 \sin \epsilon + \frac{p_1 A_1}{\tan \epsilon} \cos \epsilon - (p_2 + \rho_2 q_2^2) A_2 \sin(\epsilon - \delta)$$

$$- \frac{p_2 A_2 \cos(\epsilon - \delta)}{\tan(\epsilon - \delta)} = 0 \quad (38)$$

But from geometry it can be seen that

$$\frac{A_2}{A_1} = \frac{\sin(\epsilon - \delta)}{\sin \epsilon} \quad (39)$$

After substitution of Eqs. (40); (33), (37) and (38) become

$$\rho_2 q_2 \sin(\epsilon - \delta) - \rho_1 q_1 \sin \epsilon = 0 \quad (40)$$

$$\rho_2 q_2^2 \sin(\epsilon - \delta) \cos(\epsilon - \delta) - \rho_1 q_1^2 \sin \epsilon \cos \epsilon = 0 \quad (41)$$

$$p_2 + \rho_2 q_2^2 \sin^2(\epsilon - \delta) - p_1 - \rho_1 q_1^2 \sin^2 \epsilon = 0 \quad (42)$$

The above set of relations contains ϵ , δ , p_2 , ρ_2 , q_2 as unknown quantities, but

$$p_2 = p(s_2, q_2) ; \quad \rho_2 = \rho(s_2, q_2) \quad (43)$$

So that if one variable, say ϵ , is taken as an independent parameter the remaining unknowns (δ , q_2 , s_2) may be found by an iterative solution. These equations are, of course, formally the same as the ideal gas solution. The difference lies only in the variation of pressure etc., with entropy and velocity.

2.6.1 Iterative Solution of the Oblique Shock Relations

Rearranging Eq. (44) yields;

$$\sin(\epsilon - \delta) = \frac{\rho_1 q_1 \sin \epsilon}{\rho_2 q_2}$$

while squaring both sides of Eq. (45) and substituting the above relations yields, after simplification;

$$q_2 - q_1 \left\{ \left(\frac{\rho_1}{\rho_2} \right)^2 \sin^2 \epsilon + \cos^2 \epsilon \right\}^{1/2} = 0 \quad (44)$$

and Eq. (42) becomes

$$p_2 + \rho_1 q_1^2 \sin^2 \epsilon \left\{ \frac{\rho_1}{\rho_2} - 1 \right\} - p_1 = 0 \quad (45)$$

In functional form Eqs. (44) and (45) are just

$$\begin{aligned} G_1(s_2, q_2) &= 0 \\ G_2(s_2, q_2) &= 0 \end{aligned} \quad (46)$$

From calculus

$$\begin{aligned} dG_1 &= \frac{\partial G_1}{\partial q_2} dq_2 + \frac{\partial G_1}{\partial s_2} ds_2 \\ dG_2 &= \frac{\partial G_2}{\partial q_2} dq_2 + \frac{\partial G_2}{\partial s_2} ds_2 \end{aligned} \quad (47)$$

Now

$$\left. \begin{aligned} \frac{\partial G_1}{\partial q_2} &= 1 + q_1 \left(\frac{q_1}{q_2} \right) \left(\frac{\rho_1}{\rho_2} \right)^2 \sin^2 \epsilon \frac{\partial}{\partial q_2} (\ln \rho_2) \\ \frac{\partial G_1}{\partial s_2} &= q_1 \left(\frac{q_1}{q_2} \right) \left(\frac{\rho_1}{\rho_2} \right)^2 \sin^2 \epsilon \frac{\partial}{\partial s_2} (\ln \rho_2) \\ \frac{\partial G_2}{\partial q_2} &= p_2 \frac{\partial}{\partial q_2} (\ln p_2) - \left(\frac{\rho_1}{\rho_2} \right)^2 q_1^2 \sin^2 \epsilon \rho_2 \frac{\partial}{\partial q_2} (\ln \rho_2) \\ \frac{\partial G_2}{\partial s_2} &= p_2 \frac{\partial}{\partial s_2} (\ln p_2) - \left(\frac{\rho_1}{\rho_2} \right)^2 \sin^2 \epsilon \rho_2 \frac{\partial}{\partial s_2} (\ln \rho_2) \end{aligned} \right\} \quad (48)$$

Rather than calculate the partial derivatives numerically by perturbing the functions $\ln p_2$, $\ln \rho_2$ approximate values for these derivatives will be found by assuming that locally the gas behaves ideally, that is to say

$$\frac{\partial R_2}{\partial s_2} = \frac{\partial R_2}{\partial q_2} = \frac{\partial \gamma_2}{\partial s_2} = \frac{\partial \gamma_2}{\partial q_2} = 0$$

so that holding q_2 constant

$$\frac{\partial(\ln p_2)}{\partial s_2} \approx \frac{\partial(\ln \rho_2)}{\partial s_2} \approx \frac{1}{1 - \gamma_{in}} \quad (49)$$

and holding s_2 constant

$$\frac{\partial(\ln p_2)}{\partial q_2} \approx \gamma_2 \frac{\partial}{\partial q_2} (\ln \rho_2) \approx -\frac{q_2 \rho_2}{p_2} \quad (50)$$

writing Eq. (47) in finite difference form:^{*}

$$G_1^{(n+1)} - G_1^{(n)} = \frac{\partial G_1^{(n)}}{\partial q_2} \left(q_2^{(n+1)} - q_2^{(n)} \right) + \frac{\partial G_1^{(n)}}{\partial s_2} \left(s_2^{(n+1)} - s_2^{(n)} \right)$$

$$G_2^{(n+1)} - G_2^{(n)} = \frac{\partial G_2^{(n)}}{\partial q_2} \left(q_2^{(n+1)} - q_2^{(n)} \right) + \frac{\partial G_2^{(n)}}{\partial s_2} \left(s_2^{(n+1)} - s_2^{(n)} \right)$$

Since the root $G_1 = G_2 = 0$ is desired, $G_1^{(n+1)}$, $G_2^{(n+1)}$ are set to zero, resulting in

^{*}where n here is an iteration counter.

$$s^{(n+1)} = s^{(n)} + \left(G_2^{(n)} \frac{\partial G_1^{(n)}}{\partial q_2} - G_1^{(n)} \frac{\partial G_2^{(n)}}{\partial q_2} \right) / \left(\frac{\partial G_1^{(n)}}{\partial s_2} \frac{\partial G_2^{(n)}}{\partial q_2} - \frac{\partial G_2^{(n)}}{\partial s_2} \frac{\partial G_1^{(n)}}{\partial q_2} \right) \quad (51)$$

and

$$q_2^{(n+1)} = q_2^{(n)} - \left\{ G_1^{(n)} + \frac{\partial G_1^{(n)}}{\partial s_2} \left(s^{(n+1)} - s^{(n)} \right) \right\} / \frac{\partial G_1^{(n)}}{\partial q_2} \quad (52)$$

The iterative solution using Eqs. (51) and (52) is continued until the desired convergence of G_1 and G_2 is reached. The solution is completed by

$$\delta = \epsilon - \sin^{-1} \begin{pmatrix} \rho_1 q_1 \\ \rho_2 q_2 \end{pmatrix} \sin \epsilon \quad (53)$$

The first guess to start the solution is an ideal gas solution to the set of equations. If it is indeed an ideal gas under analysis the first guess is exact. These relations are

$$\delta = \epsilon - \tan^{-1} \left\{ \tan \epsilon \left(\frac{1}{M_1^2 \sin^2 \epsilon} + \frac{\gamma_1 - 1}{2} \right) \frac{2}{\gamma_1 + 1} \right\}$$

$$q_2 = q_1 \frac{\cos \epsilon}{\cos(\epsilon - \delta)} \quad (54)$$

$$s_2 = s_1 + \frac{R_1}{\gamma_1 - 1} \left\{ \ln \left[\frac{2\gamma_1 M_1^2 \sin^2 \epsilon - (\gamma_1 - 1)}{\gamma_1 + 1} \right] + \gamma_1 \ln \left[\frac{\tan(\epsilon - \delta)}{\tan \epsilon} \right] \right\}$$

2.7 CONTACT SURFACES

Contact surfaces or slip lines are computed utilizing the condition that the pressures and flow angles must match across the surface. The equations for pressure and flow angle developed for the wall boundary conditions are also applied at the contact surface except that the streamline slope must now be obtained iteratively utilizing the matching conditions. Equations (25) and (26) are transformed to the computational coordinates and integrated via the MacCormack operator as described in Appendix A. The predictor (first level) is applied to the high Mach number side of the slip line and the corrector (second level) is applied to the low Mach number side.

With the pressure and slope now known at the contact surface the velocity is again obtained from Eq. (35). The velocity components are then evaluated from the known slip line slope.

2.8 THERMODYNAMIC PROPERTIES

The modified Program SEAGULL handles general gases composed of various chemical species rather than a global gas. This requires thermodynamic data inputs for all participating species as well as for all vibrational levels of the various excited molecules involved in vibrational energy exchange. For these molecules it is assumed that the molecular rotation remains in equilibrium with the translational temperature but each molecule is allowed to vibrate independently, corresponding to the energy in its respective vibrational level.

Thermodynamic data are supplied to the code in the form of tabular inputs of specific heat, entropy and enthalpy for each species as a function of temperature and are taken directly from the JANAF thermochemical tables (Ref. 4).

2.9 VIBRATIONAL NONEQUILIBRIUM

To make maximum use of the current technology of finite rate formulations, the various vibrational levels of the respective excited molecules are treated as individual chemical species. In order to treat them as individual species, it is first assumed that the excited molecule can be resolved into its various vibrational levels each of which is then treated as a separate species. This assumption requires that the thermodynamic properties be separately specified for each vibrational level. It is further assumed that molecular rotation remains in equilibrium with the translational temperature but the molecules can vibrate independently of the translational temperature. Accordingly, each molecule is permitted to vibrate independently corresponding to the energy in its respective vibrational level.

Appendix A

SHOCK FITTING METHOD FOR COMPLICATED
TWO-DIMENSIONAL SUPERSONIC FLOWS

Shock Fitting Method for Complicated Two-Dimensional Supersonic Flows

Manuel D. Salas*
NASA Langley Research Center, Hampton, Va.

The floating shock fitting technique is examined. Second-order difference formulas are developed for the computation of discontinuities. A procedure is developed to compute mesh points that are crossed by discontinuities. The technique is applied to the calculation of internal two-dimensional flows with arbitrary number of shock waves and contact surfaces. A new procedure, based on the coalescence of characteristics, is developed to detect the formation of shock waves. Results are presented to validate and demonstrate the versatility of the technique.

I. Introduction

INVISCID supersonic flows are governed by a first-order quasi-linear hyperbolic system of equations. The numerical computation of these flows is complicated, because the regular solution may break down due to the nonlinearity of the governing equations. The breakdown is characterized by the appearance of surfaces, such as shock waves and vortex sheets, across which the dependent variables or their derivatives are discontinuous. During the last decade, 2 numerical techniques have emerged for the analysis of these flows. One, known as shock capturing, tries to remove the explicit computation of the discontinuities by generalizing the concept of a solution of the Euler equations to include weak solutions (i.e., discontinuities). Because the shock capturing scheme requires no special treatment to deal with discontinuities, it has become an extremely popular way of computing. However, despite its present popularity, the results obtained with this technique¹ force us to agree with Moretti's conclusion that shock capturing is a poor interpretation of a physical phenomenon, and an extremely uneconomical way of computing.³

The other technique, known as shock fitting, makes special provisions for explicitly computing the discontinuities. In essence, it locates the discontinuities and treats them as boundaries between regions where a regular solution is valid. The effectiveness and soundness of this approach has been proven for a large number of problems involving 2, 3, and 4 independent variables. However, for problems in 3 or more independent variables, the partitioning of a flowfield into regions where a regular solution is valid, can create some difficult topological problems.³ Recently, Moretti⁴ has developed a technique (reminiscent of that proposed by Richtmyer and Morton,⁵ that treats the discontinuities explicitly but does not require them as boundaries of the flow. This therefore eliminates the problems associated with partitioning the flowfield. It is this technique, known as floating shock fitting, that forms the subject matter of this paper.

To avoid unnecessary complications, the technique will be discussed in the context of a two-dimensional problem. However, to demonstrate the capabilities of the technique, results from complex flowfields are presented.

Presented as Paper at the AIAA 2nd Computational Fluid Dynamics Conference, submitted June 20, 1975; revision received September 17, 1975.

Index categories: Nozzle and Channel Flow; Shock Waves and Denotations; Supersonic and Hypersonic Flow.

*Aero-Space Technologist, Aerodynamic Analysis Section, Hypersonic Aerodynamics Branch, High-Speed Aerodynamics Division. Member AIAA.

II. Problem Definition

We will discuss the floating shock fitting technique as it applies to the flow of an inviscid, perfect gas through a two-dimensional duct of arbitrary geometry. The flow is assumed to be supersonic throughout, and consequently, irregular shock reflections are not considered. Shock waves generated by either discontinuities in the slopes of the walls, or by coalescence of pressure waves, will be automatically detected and fitted into the calculation. The number of shock waves, contact surfaces, and the number of interactions of these discontinuities, is considered arbitrary (limited only by computer storage).

III. Governing Equations

The flow variables are nondimensionalized by scaling the pressure, density, and temperature, with respect to their initial values (ρ_0, ρ_0, T_0), scaling the velocities with respect to $(\rho_0 / \rho_0)^{1/2}$, and scaling all lengths with respect to some arbitrary reference length. The Euler equations written in a Cartesian frame (r, z), with the z -axis running along the length of the duct, are

$$\begin{aligned} P_r + (uwP_r + \gamma wu_r - \gamma uw_r) / \beta &= 0 \\ w_r + (uww_r - \gamma Tu_r - TuP_r) / \beta &= 0 \\ u_z + (uu_r + TP_r) / w &= 0 \\ S_z + uS_r / w &= 0 \end{aligned} \quad (1)$$

Where P is the natural logarithm of pressure, u and w are the velocity components in the r and z directions, respectively; S is the entropy, γ is the ratio of specific heats; the temperature is given by

$$T = \exp((S + (\gamma - 1)P) / \gamma) \quad (2)$$

$$\text{and } \beta = w^2 - \gamma T.$$

The following equations are introduced here for later reference. By combining the 2 momentum equations, we get

$$\tau_z + \frac{w^2 \tau \tau_r}{\beta} + \left(I + \frac{\tau^2 w^2}{\beta} \right) \frac{TP_r}{w^2} = 0 \quad (3a)$$

where $\tau = u / w$. With Eq. (3a) and the continuity equation in the form

$$P_z + w^2 (\tau P_r + \gamma \tau_r) / \beta = 0 \quad (3b)$$

we can obtain the compatibility equation

$$\tau' \pm ([\gamma T(\beta + w^2 \tau^2)]^{1/2} / \gamma w^2) P' = 0 \quad (4)$$

where the primes denote differentiation along the characteristic directions

$$\lambda^\pm = (w^2 \tau \pm [\gamma T(\beta + w^2 \tau^2)]^{1/2}) / \beta \quad (5)$$

The Euler Eqs. (1) are recast in terms of computational coordinates (X, Z) defined by

$$X = (r - b(z)) / (c(z) - b(z)) \quad Z = z \quad (6)$$

where $r = b(z)$ and $c(z)$ define the lower and upper walls of the duct. In matrix form the equations of motion become

$$f_Z = \underline{A} f_X \quad (7)$$

where the vector f is

$$f = \begin{bmatrix} P \\ u \\ w \\ S \end{bmatrix} \quad (8)$$

and the matrix \underline{A} is

$$\underline{A} = \begin{bmatrix} a_{11} & a_{12} & a_{13} & 0 \\ a_{21} & a_{22} & 0 & 0 \\ a_{31} & a_{32} & a_{11} & 0 \\ 0 & 0 & 0 & a_{22} \end{bmatrix} \quad (9)$$

$$\begin{aligned} a_{11} &= -(uwX_r + \beta X_z) / \beta \\ a_{12} &= -\gamma w X_r / \beta \\ a_{13} &= \gamma u X_r / \beta \\ a_{21} &= -TX_r / w \\ a_{22} &= -(uX_r + wX_z) / w \\ a_{31} &= u TX_r / \beta \\ a_{32} &= \gamma TX_r / \beta \end{aligned}$$

IV. Interior Point Computation

Unlike shock fitting, floating shock fitting does not subdivide the computational plane into regions bounded by discontinuities; instead, a single region is used, as illustrated in Fig. 1. In this single region, mesh points are equally spaced, and all discontinuities are allowed to move freely or float over the fixed grid. Their motion is subject only to the governing equations.

Except for the mesh points at the walls and in the neighborhood of a discontinuity, all mesh points are computed using the MacCormack scheme⁶ to integrate Eq. (7). For example, consider the section of a duct, in the computational plane, sketched in Fig. 1. Using the MacCormack scheme, and assuming the solution is known at the K th steps, $f_{N,K+1}$ is obtained from

level 1

$$f_{N,K+1} = f_{N,K} + \underline{A}_{N,K} (f_{N+1,K} - f_{N,K}) \Delta Z / \Delta X$$

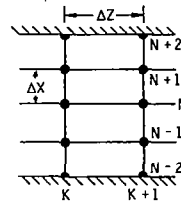


Fig. 1 Computational plane.

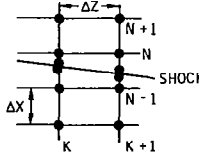


Fig. 2 Computation in the neighborhood of a shock wave.

level 2

$$\begin{aligned} f_{N,K+1} &= \frac{1}{2} (f_{N,K} + \tilde{f}_{N,K+1} + \underline{A}_{N,K+1} \\ &\quad (\tilde{f}_{N,K+1} - \tilde{f}_{N-1,K+1}) \Delta Z / \Delta X) \end{aligned} \quad (10)$$

Because the discontinuities are allowed to float over the fixed grid, special provisions must be taken when evaluating the X derivatives of f , at mesh points in the neighborhood of a discontinuity. Consider again the computation of point $(N, K+1)$, but now in the presence of a shock as shown in Fig. 2. There is no difficulty in computing the first level of the MacCormack scheme, since the forward difference

$$f_X = (f_{N+1,K} - f_{N,K}) / \Delta X$$

is valid. However, for the second level, the backward difference

$$\tilde{f}_X = (\tilde{f}_{N,K+1} - \tilde{f}_{N-1,K+1}) / \Delta X$$

is not allowed because \tilde{f} is not differentiable across the shock. On the other hand, the very simple approximation,

$$\tilde{f}_X = (\tilde{f}_{N,K+1} - \tilde{f}_{S,K+1}) / (X_N - \bar{X}_{S,K+1})$$

where S denotes conditions at the shock, can result in large truncation errors, and the computation becomes unstable. Moretti recommends using an approximation that involves the values at the shock and the 3 neighboring mesh points [Eq. (61) in Ref. 2]. We have not used this approximation, because it makes the numerical domain of dependence point $(N, K+1)$ much larger than it physically is. Instead, we use the following approximation

$$\begin{aligned} \tilde{f}_X &= -[(0.5\epsilon - 1)\tilde{f}_{N+1,K+1} + 0.5\tilde{f}_{S,K+1} \\ &\quad + 0.5(1-\epsilon)\tilde{f}_{N,K+1}] / \Delta X \end{aligned} \quad (11)$$

where

$$\epsilon = (X_{N,K+1} - \bar{X}_{S,K+1}) / \Delta X$$

The truncation error for Eq. (11), (based on f_X , not f) is given by

$$(\epsilon+2)(\epsilon-1)\Delta X / 4f_{XX}$$

With Eq. (11), the computation of point $(N, K+1)$ proceeds as the computation of any other interior point. Similar considerations apply to the computation of point $(N-1, K+1)$.

If point $(N+1, K+1)$ is not available when applying Eq. (11), as is the case indicated in Fig. 3 where 2 shocks are

Fig. 3 Computation with closely spaced shocks.

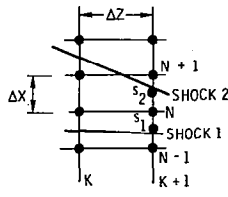
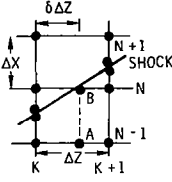


Fig. 4 Computation when a shock crosses a mesh line.



shown close to each other, then if the distance between the shocks is greater than ΔX , f_X is approximated by

$$f_X = (\tilde{f}_{s2,K+1} - \tilde{f}_{s1,K+1}) / (\tilde{X}_{s2,K+1} - \tilde{X}_{s1,K+1}) \quad (12)$$

If, however, the distance between the shocks is smaller than ΔX , the values at $(N, K+1)$ are interpolated from the shock values.

When a discontinuity crosses a mesh line, the computation of this mesh point must be modified. In Fig. 4, an up-running shock is shown crossing the N th mesh line between steps K and $K+1$. The usual interior point computation would require taking the one-sided difference between points $(N+K, K)$ and (N, K) for level one. This procedure is no longer proper, because of the presence of the shock. We, therefore, proceed by evaluating points A and B as follows

$$\left. \begin{aligned} f_A &= f_{N-1,K} + \delta(\tilde{f}_{N-1,K+1} - f_{N-1,K}) \\ f_B &= f_{s,K} + \delta(\tilde{f}_{s,K+1} - f_{s,K}) \end{aligned} \right\} \quad (13)$$

where

$$\delta = (X_N - X_{s,K}) / (\tilde{X}_{s,K+1} - X_{s,K}) \quad (14)$$

then, the value of f for level one at $(N, K+1)$ is

$$f_{v,K+1} = f_B + A_B(f_B - f_A)(1 - \delta)\Delta Z / \Delta X \quad (15)$$

Care must be taken in evaluating δ when $dX_s/dZ \approx 0$, since Eq. (14) becomes indeterminate. We therefore require that,

$$\left| \frac{dX_s}{dZ} \right| \Delta Z > 0.2 \Delta X$$

otherwise, δ is set to one to give the desired result

$$\tilde{f}_{N,K+1} = \tilde{f}_{s,K+1}$$

A similar computation is performed when a down-running discontinuity crosses a mesh line.

V. Wall Computation

The compatibility equation, Eq. (4), is applied at the wall to evaluate P_Z

$$P_Z = -\partial P_X^\pm / \left[\gamma T(\beta + w^2 \tau^2) \right]^{1/2} (\tau_Z + \lambda \tau_X) \quad (16)$$

where

$$\lambda = X_z + \lambda^\pm X_r$$

Here, the X derivatives are evaluated as three-point one-sided differences and

$$\tau_Z = \begin{cases} b_{zz} \text{ for } \lambda^- \\ c_{zz} \text{ for } \lambda^+ \end{cases}$$

Then, following the MacCormack algorithm, the value of the pressure at the wall, P_w , is given by

$$\begin{aligned} \tilde{P}_{w,K+1} &= P_{w,K} + P_Z \Delta Z \\ P_{w,K+1} &= \frac{1}{2} (P_{w,K} + \tilde{P}_{w,K+1} + \tilde{P}_Z \Delta Z) \end{aligned}$$

With the pressure and entropy known at the wall, the temperature is obtained from Eq. (2), and the magnitude of the velocity from

$$\frac{u^2 + w^2}{2} + \frac{\gamma}{\gamma - 1} T = \text{constant} \quad (17)$$

The two-velocity component can then be determined from the known wall slope and the vanishing of the velocity component normal to the wall.

VI. Shock Detection

Perhaps the most distinguishing feature of the problem we are considering, and certainly its most troublesome one, is the possible formation of shock waves. In this section, we will consider the procedure required to detect an incipient shock. There are two important features for any such procedure. First, the procedure must be reliable. Incipient shocks must be located at the proper place, but most important, the procedure must be able to interpret the physics of the problem accurately, and should not be so sensitive as to create nonexistent shocks. Secondly, because the procedure must be executed at every step, it must be very fast and require a minimum amount of data to make a reliable decision.

The procedure we have constructed, based on the concept of coalescing characteristics, requires only information on 2 adjacent mesh points, and we find it to be both reliable and fast. However, its empirical nature should be kept in mind. It is applied at the end of a computational step as follows:

Assume that the flowfield is known at the K th step (see Fig. 5). At each mesh point N and $N-1$, the up-running ($\lambda_N^+, \lambda_{N-1}^+$) and downrunning ($\lambda_N^-, \lambda_{N-1}^-$) characteristics are evaluated using Eq. (5). If we now assume that the ΔZ intervals between steps (evaluated from the CFL condition)^a are essentially the same, then a quantity η^\pm , which is the reciprocal of the number of steps needed for 2 characteristics to coalesce can be evaluated from

$$\eta^\pm = (\lambda_{N-1}^\pm - \lambda_N^\pm) \Delta z / \Delta r$$

A considerable number of numerical experiments indicate that a shock should be fitted into the calculation when η^\pm becomes greater than 0.22 (approximately 4 steps before the characteristics coalesce).

We have found that for a wide range of problems, if the detection of incipient shocks is delayed until $\eta^\pm < 0.22$, then the procedure becomes very sensitive and shocks are predicted unnecessarily.

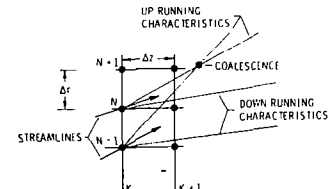


Fig. 5 Details of the shock detection.

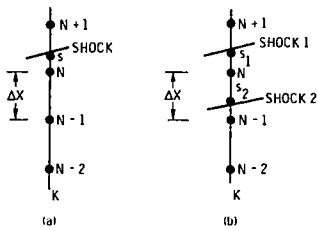


Fig. 6 Evaluation of the low-pressure side of a shock.

The detected shock is assumed to have the average slope of the coalescing characteristics and to be located half way between r_N and r_{N-1} . With the initial shock location known, the initial flow variables on the low pressure side are linearly interpolated between the 2 mesh points bracketing the shock, and on the high pressure side they are linearly extrapolated using the 2 mesh points next to the shock on the high pressure side.

Shocks that are generated at the walls of the duct, because of slope discontinuities at the walls, are introduced from user supplied information on the wall geometries, and do not make use of the procedure described in this section.

VII. Shock Computation

The low-pressure side of a shock is computed using the same scheme described for the interior point computation, but using the X derivatives given in this section. In Fig. 6, assuming that mesh point N lies on the low-pressure side, the X derivatives at the shock for the predictor level are evaluated from

$$f_{X_s} = \left[\frac{2}{1+\epsilon} (f_{s,K} - f_{N-1,K}) + 0.5 f_{N-2,K} - \frac{(0.5+\epsilon)}{(1+2\epsilon)} f_{N,K} \right] / \Delta X \quad (18)$$

where

$$\epsilon = (X_{s,K} - X_{N,K}) / \Delta X \quad (19)$$

If only two mesh points are available, then the derivatives are evaluated from

$$f_{X_s} = \left[-\frac{2\epsilon-1}{1+\epsilon} f_{N-1,K} + \frac{3}{1+\epsilon} f_{s,K} - 2f_{N,K} \right] / \Delta X \quad (20)$$

with ϵ given by Eq. (19). The truncation error for Eq. (18) is of order ΔX^2 and for Eq. (20) it is

$$(\epsilon-1) \frac{\Delta X}{2} f_{XX_s}$$

It should be noted that Eqs. (18-20) are not the same formulas suggested by Moretti,^{2,4} particularly Eq. (18) has a lower truncation error than Moretti's counterpart.

If only 1 mesh point is available (Fig. 6b), then f_{X_s} is approximated by

$$f_{X_s} = (f_{s,K} - f_{s,2,K}) / (X_{s,1,K} - X_{s,2,K}) \quad (21)$$

provided that $(X_{s,1,K} - X_{s,2,K})$ is greater than ΔX . If $(X_{s,1,K} - X_{s,2,K})$ is smaller than ΔX , then f_{X_s} is set to zero. For the corrector stage, the same derivatives are used but with f replaced by \bar{f} .

If the low-pressure side lies on the other side of the shock, the derivatives that are used are the negatives of those given by Eq. (18) and Eq. (20), and ϵ is given by the negative of Eq. (19).

The computation of the high-pressure side of the shock has been formulated using the compatibility equation, Eq. (4), on the characteristic reaching the shock on the high-pressure side along with Rankine-Hugoniot conditions. The details of this classical treatment of the shock can be found in Ref. 4.

The computation of the high-pressure side was the only computation requiring involved programming logic. The main difficulty is the determination of the origin of the characteristic reaching the shock in the immediate vicinity of other discontinuities. It should be, however, possible to avoid these difficulties by computing the high-pressure side with the method suggested by Kentzer.⁷

VIII. Contact Surface Computation†

To compute a contact surface, we exploit the fact that both pressure and streamline slope are continuous across a contact surface. Eqs. (3a, b), which involve derivatives of P and τ only, are thus recast in terms of the computational coordinates (X, Z), and are integrated using the MacCormack scheme where the X derivatives are evaluated using Eq. (20). In the predictor level, Eq. (20) is applied on the high Mach number side of the contact surface. In the corrector level, it is applied on the low Mach number side. This choice is arbitrary, and the same results are obtained if the order is reversed.

With the pressure and entropy known at the contact surface, the magnitude of the velocity follows from Eq. (17), and the 2 velocity components can be determined from the evaluated streamline slope.

IX. Interactions

The interactions of the discontinuities with the walls of the duct and with each other are computed by locally exact solutions. The details of these calculations can be found in most text books in fluid mechanics, for example, Ref. 8, and will not be discussed here.

X. Elimination of Weak Discontinuity

Discontinuities with a Mach number difference across the discontinuity of less than 1% are automatically eliminated from the computation. This feature is not a requirement of the technique. It has, however, been incorporated, because for most practical applications, tracing these weak discontinuities is not necessary. It speeds up the computation, and it avoids computing degenerate discontinuities (i.e. the contact surface formed by the interaction of 2 shock waves of equal strength).

XI. Results

The results of several calculations performed with the floating shock fitting technique are presented to demonstrate the accuracy and versatility of the technique. All the computations were done on a CDC 6600 computer. The core required to run the code is under 55000₈ locations.

The flowfield produced by a uniform flow impinging on a wedge is often used to validate numerical calculations. The problem is a trivial one, consisting of uniform properties in front and behind the shock wave. The exact solution for a freestream Mach number of 3.50 which is initially compressed by a 15° wedge and then expanded, such as to exactly cancel the shock wave generated by the wedge, is shown in Fig. 7. In the figure, the lower wall pressure distribution shown corresponds to the case where the expansion occurs a very short distance before the shock reflects from the wall. The exact solution is obtained with the floating shock fitting

†We have recently experienced some difficulties with this procedure when the contact surface is next to a strong expansion fan. The problems have been overcome by reformulating the contact surface computation along the guide lines discussed in the shock computation.

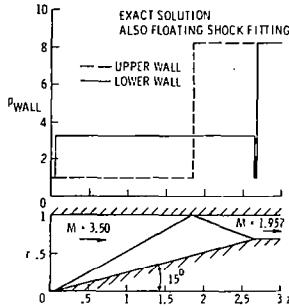


Fig. 7 Flowfield over a 15° wedge with shock cancellation.

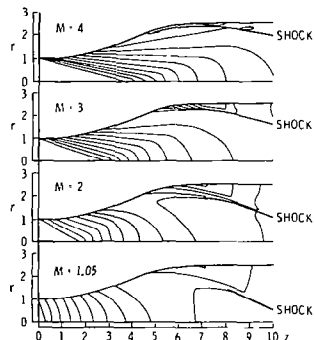


Fig. 8 Parametric study of a nozzle, showing shock waves and isobars.

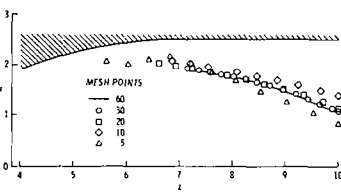


Fig. 9 Shock path for $M = 1$ case.

technique using only 2 mesh points in less than 1 sec of computational time (the same results are obtained increasing the number of mesh points).

In Fig. 8, the results of a parametric study of the flowfield produced by a nozzle are presented. The initial Mach number was used as the parameter, allowing it to range from near 1 to 4. Both the isobars and shock-wave patterns are shown in the figure. For the Mach 4 case, most of the isobars downstream of the shock wave were not included in the figure to avoid overcrowding of lines. The total computational time for these 4 cases, using 30 mesh points, was approximately 25 sec. Figures 9 and 10 give some further details in the calculation of the Mach 2 case. In these 2 figures the results obtained with 5, 10, 20, 30, and 60 points are shown. Figure 9 shows the calculated shock-wave path, while Fig. 10 shows the upper wall pressure distribution. The results show that a good qualitative result for this more complicated problem can be obtained with as few as 5 mesh points, and that good quantitative results are obtained with only 10 mesh points.

It is very often argued that shock fitting is limited in its capability to handle flowfields with more than a single shock.⁹⁻¹¹ In Refs. 3 and 12 this has been shown not to be the case for very complex three-dimensional steady, and one-dimensional time-dependent flows. We hope to fill the existing gap for two-dimensional steady problems with Fig. 11 and also to demonstrate that floating shock fitting is a numerically stable technique even in multishocked flowfields. In Fig. 11, the geometry of NASA Langley's scramjet combustor model is simulated. The results shown are for a flow with an incoming Mach number equal to 3, inclined at 8° with the horizontal. The resulting flowfield con-

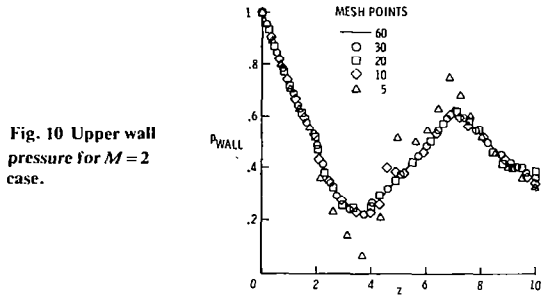


Fig. 10 Upper wall pressure for $M = 2$ case.

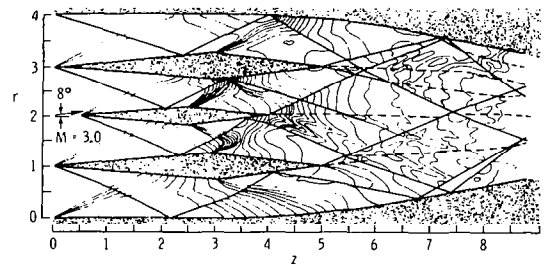


Fig. 11 Flowfield for a simulated scramjet, showing shock waves, vortex sheets and isobars.

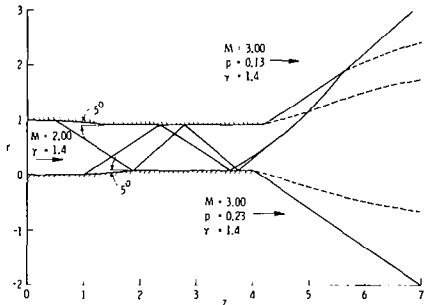


Fig. 12 Plume flowfield showing shock waves and vortex sheets.

sists of a complex pattern of interacting expansions and shock waves. In the figure, the shock-wave pattern is shown by the heavy lines. The contact surfaces are shown by the dashed lines, and isobars are shown by the light lines. Certain discontinuities are seen to terminate abruptly in the flowfield, while some shock interactions do not show the expected vortex sheet; this is a result of the automatic elimination of weak discontinuities previously discussed. The calculation was performed in 6 pieces, using a total of 120 mesh points and requiring approximately 2.2 min of computational time. The calculation shows approximately a dozen discontinuities, with some 40 interactions.

The technique has been extended to internal axisymmetric flows (with and without swirl), internal line source type flows, and to external two-dimensional flows. An example of the application to external flows is shown in Fig. 12, where a flow with an initial Mach number of 2.0 exhausts into a Mach 3.0 freestream. The lower wall ends at $z=4.0$, while the upper wall ends at $z=4.2$. The freestream conditions for the external flows are shown in the figure.

XII. Conclusions

Floating shock fitting for two-dimensional steady flows is an accurate and stable technique capable of solving very-complex problems with acceptable running times. A fully three-dimensional code is planned for the near future.

References

¹ Moretti, G., "Three-Dimensional, Supersonic, Steady Flows With Any Number of Imbedded Shocks," AIAA Paper 74-10, Washington, D.C., 1974.

² Moretti, G., "Experiments in Multi-Dimensional Floating Shock Fitting," Polytechnic Institute of Brooklyn, PIBAL Rept. 73-18, Aug. 1973.

³ Marconi, F. and Salas, M., "COMPUTATION OF Three-Dimensional Flows About Aircraft Configurations," *Computers and Fluids*, Vol. 1, 1973, pp. 185-195.

⁴ Moretti, G., "Thoughts and Afterthoughts About Shock Computations," Polytechnic Institute of Brooklyn, PIBAL Rept. 72-37, Dec. 1972.

⁵ Richtmyer, R.D. and Morton, K.W., *Difference Methods for Initial-Value Problems*, Interscience Publishers, New York, 1967, p. 378.

⁶ MacCormack, R.W., "The Effect of Viscosity in Hypervelocity Impact Cratering," AIAA Paper 69-354, Cincinnati, Ohio, 1969.

⁷ Kentzer, C., "Discretization of Boundary Conditions on Moving Discontinuities," *Proceedings of the Second Int. Conf. on Numerical Methods in Fluid Dynamics*, Berkeley, Calif., Sept. 1970, pp. 108-113.

⁸ Courant, R. and Friedrichs, K.O., *Supersonic Flow and Shock Waves*, Interscience Publishers, Inc., New York, Chapt. III.

⁹ Vinokur, M., "Conservation Equations of Gasdynamics in Curvilinear Coordinate Systems," *Journal of Computational Physics*, Vol. 14, 1974, pp. 105-125.

¹⁰ Kutler, P., Lomax, H., and Warming, R.F., "Computation of Space Shuttle Flow Fields Using Non-Centered Finite-Difference Schemes," AIAA Paper 72-193, San Diego, Calif., 1972.

¹¹ Kutler, P., and Reinhardt, W.A., "Numerical Computation of Multi-Shocked Three-Dimensional Supersonic Flow Fields With Real Gas Effects," AIAA Paper 72-702, Boston, Mass., 1972.

¹² Moretti, G., "Complicated One-Dimensional Flows," Polytechnic Institute of Brooklyn, PIBAL 71-25, Sept. 1971.

Appendix B
INPUT GUIDE AND SAMPLE CASES

Appendix B
INPUT GUIDE AND SAMPLE CASES

DESCRIPTION OF INPUT DATA

ALL INPUT DATA IS READ FROM TAPE 5.

*THE FIRST INPUT CARD CONSISTS OF 11 INTEGERS.
THE FORMAT IS 16I5
THESE INTEGERS ARE ID, KOUT, ICN, IBN, ISO, NA, ISY, JJ, ITY, ITP, IVI
ITY IS USED TO INDICATE MERGING OF INTERNAL DUCTS, AND IS NOT
RELATED TO JETS OR PLUMES.

ID=0 INPUT CARD NO. 3 IS NOT READ
ID=1 INPUT CARD NO. 3 IS READ
KOUT = THE NO. OF STEPS TAKEN BEFORE A COMPLETE OUTPUT OF
THE FLOW FIELD IS MADE
ICN = THE TOTAL NO. OF SHARP CORNERS ON THE UPPER WALL
ICN CANNOT EXCEED 10
IBN = THE TOTAL NO. OF SHARP CORNERS ON THE LOWER WALL
IBN CANNOT EXCEED 10
ISO=0 NO ISOBAR OUTPUT WILL BE PROVIDED
ISO=1 ISOBARS WILL BE COMPUTED AND PRINTED AT EVERY STEP
NA = INITIAL NUMBER OF MESH POINTS MINUS TWO
NA CANNOT EXCEED 98
IN MOST CASES 20 POINTS ARE SUFFICIENT, AND ON THE AVERAGE
THERE SHOULD BE ABOUT 5 POINTS BETWEEN DISCONTINUITIES.
ISY=0 NO SYMMETRY IS ASSUMED IN THE COMPUTATION OF THE LOWER
WALL
ISY=1 SYMMETRY IS IMPOSED IN THE COMPUTATION OF THE LOWER WALL
JJ=0 FOR TWO DIMENSIONAL FLOW
JJ=1 FOR AXISYMMETRIC FLOW
JJ=2 FOR LINE SOURCE FLOW
ITY=0 A SINGLE DUCT CALCULATION
ITY=1 SINGLE DUCT CALCULATION WITH DATA WRITTEN ON TAPE 7
FOR FUTURE MERGING RUN. CAN ALSO BE USED TO RESTART
A CALCULATION
ITY=2 DATA IS READ TO MERGE TWO OR MORE FLOWS, AND DATA IS
WRITTEN ON TAPE 7 FOR FUTURE CONTINUATION
ITY=3 DATA IS READ TO MERGE TWO OR MORE FLOWS
ITP=0 NO CALCOMP PLOT IS GENERATED
ITP=1 A CALCOMP PLOT IS GENERATED
IVI=0 NO VISCOUS FORCES ARE COMPUTED
IVI=1 SPALDING-CHI USED TO COMPUTE VISCOUS FORCES, THE
REYNOLDS NO. WILL BE BASED ON THE WALL GEOMETRY
LENGTH

*INPUT CARD NO. 2 CONSISTS OF 5 INTEGERS

THE FORMAT IS 16I5

NS = NO. OF CHEMICAL SPECIES

NT = NO. OF POINTS IN THERMODYNAMIC TABLES

NM = NO. OF CATALYTIC SPECIES

NR = NO. OF REACTIONS IN MECHANISM

IFROZE=0, FINITE RATE

IFROZE=1, FROZEN FLOW

*INPUT CARD NO. 3 IS READ ONLY IF ID=1

ITS PURPOSE IS SOLELY FOR IDENTIFICATION, A FREE FIELD FORMAT
IS USED BETWEEN COLUMNS 6 THRU 55

*INPUT CARD NO. 4 CONSISTS OF 5 FLOATING POINT NUMBERS

THE FORMAT IS 8E10.4

THESE NUMBERS ARE ACH, GM, DIST, TOLER, SCALE

ACH = INITIAL MACH NUMBER

GM = RATIO OF SPECIFIC HEATS

DIST = DISTANCE TO THE END OF THE CALCULATION (CM)

TOLER = A TOLERANCE PARAMETER TO INCREASE OR DECREASE THE
NO. OF MESH POINTS. IT WORKS AS FOLLOWS: IF SET TO X
THEN THE NO. OF MESH POINTS WILL BE INCREASED WHEN
THE DISTANCE BETWEEN MESH POINTS IS X TIMES THE INITIAL
DISTANCE BETWEEN MESH POINTS, AND MESH POINTS ARE DE-
CREASED WHEN THE DISTANCE BETWEEN MESH POINTS IS 1./X
TIMES THE INITIAL DISTANCE BETWEEN MESH POINTS.

SETTING TOLER TO A LARGE NUMBER (SAY 1000.) HAS THE
EFFECT OF NOT CHANGING THE NUMBER OF MESH POINTS.

SCALE = IS A SCALE FACTOR FOR CALCOMP PLOTS NEEDED ONLY IF
ITP=1 BOTH THE R AND Z COORDINATES ARE MULTIPLIED
BY SCALE BEFORE THEY ARE PLOTTED.

*INPUT CARD NO. 5 CONSISTS OF 7 FLOATING POINT NUMBERS

THE FORMAT IS 8E10.4

THE NUMBERS ARE ZEXIT, PINF, TINF, GMINF, ACHINF, ANGINF, RCINF
THIS INFORMATION IS NEEDED IN CASE THE LOWER WALL OF THE DUCT
OPENS TO THE FREE STREAM AT Z=ZEXIT. IF THIS IS NOT THE CASE
THEN ZEXIT SHOULD BE SET TO A NUMBER GREATER THAN THE VALUE
OF DIST, AND THE REMAINING SIX NUMBERS NEED NOT BE DEFINED.

ZEXIT = LOCATION OF EXIT PLANE (CM)

PINF = FREE STREAM STATIC PRESSURE (ATM)

TINF = FREE STREAM STATIC TEMPERATURE (°K)

GMINF = NOT REQUIRED PRESENTLY

ACHINF = FREE STREAM MACH NUMBER

ANGINF = FREE STREAM INCLINATION IN DEGREES, MEASURED POSITIVE
COUNTERCLOCKWISE FROM THE Z AXIS

RCINF = NOT REQUIRED PRESENTLY

*INPUT CARD NO. 6 (REQUIRED ONLY IF ZEXIT. LE. DIST)
THE FORMAT IS 8E10.4
THIS CARD SUPPLIES THE SPECIES DISTRIBUTION IN THE EXTERNAL
STREAM IN THE SAME ORDER AS IN THE MAIN STREAM*

ALFA(1, 1), FIRST SPECIES IN THERMO DATA TABLES
ALFA(2, 1), SECOND SPECIES IN THERMO DATA TABLES
ALFA(N, 1), N-TH SPECIES IN THERMO DATA TABLES

*INPUT CARD NO. 7 IS THE SAME AS CARD NO. 5, BUT FOR THE CASE
WHEN THE UPPER WALL OF THE DUCT OPENS TO FREE STREAM.

*INPUT CARD NO. 8 IS THE SAME AS CARD NO. 6 BUT FOR THE CASE
WHEN THE UPPER WALL OF THE DUCT OPENS TO FREE STREAM.

*INPUT CARD NO. 9 CONSISTS OF ICN FLOATING POINT NUMBERS, IF
ICN=0 THE INPUT CARD IS NOT NEEDED. THESE NUMBERS ARE
STORED IN ARRAY ZIC(N).
THE FORMAT IS 8E10.4

ZIC(N) = LOCATION OF THE NTH CORNER ON THE UPPER WALL (CM)

*INPUT CARD NO. 10 CONSISTS OF ICN FLOATING POINT NUMBERS, IF
ICN=0 THE INPUT CARD IS NOT NEEDED. THESE NUMBERS ARE STORED
IN ARRAY AIC(N).
THE FORMAT IS 8E10.4

AIC(N) = THE CHANGE IN ANGLE IN DEGREES AT THE NTH UPPER WALL
CORNER. AIC IS DEFINED POSITIVE IF THE CORNER IS A COM-
PRESSION AND NEGATIVE IF AN EXPANSION. NOTE THAT IT IS
A CHANGE IN ANGLE AND NOT THE NEW WALL ANGLE.

*INPUT CARD NO. 11 IS THE SAME AS CARD NO. 6, BUT FOR THE LOWER
WALL. THE DATA IS STORED IN ARRAY ZIB(N), THE INPUT CARD IS NOT
NEEDED IF IBI=0.

*INPUT CARD NO. 12 IS THE SAME AS CARD NO. 7, BUT FOR THE LOWER
WALL. THE DATA IS STORED IN ARRAY AIB(N), THE INPUT CARD IS NOT
NEEDED IF IBI=0. AIB IS DEFINED IN THE SAME WAY AS AIC.

*INPUT CARD NO. 13 CONSISTS OF 6 FLOATING POINT NUMBERS
THIS CARD IS NOT NEEDED IF IVI=0
THE FORMAT IS 8E10.4

ATWTI(1) = NONDIMENSIONAL LOWER WALL TEMPERATURE
ATWTI(2) = NONDIMENSIONAL UPPER WALL TEMPERATURE
XL(1) = LOWER WALL VIRTUAL ORIGIN FOR SPALDING-CHI (GREATER
THAN 0.)
XL(2) = UPPER WALL VIRTUAL ORIGIN FOR SPALDING-CHI (GREATER
THAN 0.)
REI = REYNOLDS NO. PER UNIT LENGTH
PRAND = PRANDTL NO.

*IF PARTICULAR SPECIES DOES NOT EXIST ENTER ZERO IN THAT LOCATION.

*INPUT CARD NO. 14 INITIAL PRESSURE AND TEMPERATURE IN INTERNAL DUCT.
THE FORMAT IS 8E10.4

PIN = INITIAL PRESSURE (ATM)
TIN = INITIAL TEMPERATURE ($^{\circ}$ K)

*INPUT CARD(S) NO. 15 SPECIES DISTRIBUTION MOLE FRACTION IN INTERNAL DUCT.

ALFA(1, 1), FIRST SPECIES IN THERMO DATA TABLES
ALFA(2, 1), SECOND SPECIES IN THERMO DATA TABLES
ALFA(N, 1), NTH SPECIES IN THERMO DATA TABLES

*INPUT CARD(S) NO. 16 SPECIES ID AND THERMODYNAMIC DATA
THE FORMAT IS A6, 2E10.3

AID(I), ITH SPECIES IDENTIFICATION
WTM(I), ITH SPECIES MOLECULAR WEIGHT (g/g-mole)
HF(I), ITH SPECIES HEAT OF FORMATION (K-cal/mole)
TTB(J), JTH TEMPERATURE POINT IN TABLES (K)
CPTB(1, J) SPECIFIC HEAT FOR ITH SPECIES AT JTH TEMPERATURE POINT (cal/mole-K)
STB(K, J) ENTROPY FOR ITH SPECIES AT JTH TEMPERATURE POINT (cal/mole-K)
HTB(I, J) ENTHALPY FOR ITH SPECIES AT JTH TEMPERATURE POINT (K-cal/mole)

*INPUT CARD(S) NO. 17 CATALYTIC SPECIES DATA (OPTIONAL) INPUT ONLY IF NM=0
THE FORMAT IS A6/(16E5.2)
IF NM \neq 0, INPUT THE FOLLOWING
AID(J), NAME OF JTH CATALYTIC SPECIES
WF(J, K), WEIGHTING FACTOR OF ITH SPECIES FOR JTH CATALYTIC SPECIES

AID(J), NAME OF JTH CATALYTIC SPECIES
WF(J, I), WEIGHTING FACTOR OF ITH SPECIES FOR JTH CATALYTIC SPECIES

*INPUT CARD NO. 18 NAME OF REACTION SET
THE FORMAT IS 13A6, A2

*INPUT CARD NO. 19 REACTION RATE DATA (OPTIONAL) INPUT ONLY IF IFROZE IS ZERO
THE FORMAT IS A6, 1X, A6, 1X, A6, 1X, A6, 1X, A6, 1X, A6, 7X, 12, 11, E8.2, F5.2, F10.1, 1F6.2

AID(J), SPECIES (NAME) APPEARING IN ITH REACTION
IRR(I), REACTION TYPE
IRT(I), RATE CONSTANT TYPE
RCT(I, N), RATE CONSTANT COEFFICIENTS $N = 1, 4$

^{*}

FOR MOST RUNS, WITH THE EXCEPTION OF CASES WHERE ITY=2 OR ITY=3, THIS IS ALL THE INFORMATION REQUIRED AS INPUT DATA. CASES WHERE ITY=2 OR ITY=3 WILL BE DISCUSSED LATER. LET US CONSIDER NOW THE DEFINITION OF THE WALL GEOMETRIES.

THE LOWER WALL GEOMETRY SHOULD BE DEFINED IN SUBROUTINE GEOMB. THE USER DEFINES THE GEOMETRY BY GIVING R OF THE WALL AS A FUNCTION OF THE AXIAL COORDINATE Z. THE CODE ASSUMES THAT THE INITIAL STATION IS AT Z=0. IF IT IS NECESSARY TO START THE CALCULATION AT SOME OTHER VALUE OF Z, THIS CAN BE DONE BY REDEFINING Z IN THE MAIN PROGRAM. IN ADDITION THE FIRST DERIVATIVE, RZ, AND THE SECOND DERIVATIVE, RZZ, ARE ALSO REQUIRED.

THE UPPER WALL GEOMETRY SHOULD BE DEFINED IN SUBROUTINE GEOMC. THE GEOMETRY IS DEFINED IN THE SAME MANNER AS DESCRIBED ABOVE. A SAMPLE UPPER GEOMETRY FOR A DUCT WITH AN INITIAL HEIGHT OF ONE UNIT, A 10. DEGREE COMPRESSION AT Z=.5 AND A 6 DEGREE EXPANSION AT Z=1. IS:

```
R=1. $ RZ=0. $ RZZ=0. $ IF (Z.LT.0.5) RETURN
R=1. -.17633*(Z-.5) $ RZ=-.17633 $. RZZ=0.
IF (Z.LT.1.) RETURN
R=.911835+.1051*(Z-1.) $ RZ=.1051 $ RZZ=0. $ RETURN
```

CARE SHOULD BE EXERCISED WHEN DEFINING WALL GEOMETRIES, AS THE MOST FREQUENT CAUSE OF PROBLEMS THAT USERS HAVE EXPERIENCED WITH THIS PROGRAM IS USUALLY RELATED TO IMPROPER GEOMETRY DEFINITION.

*The pre-exponential factor, N = 1, has units of (cm-particle-sec). The activation energy, N = 3, has the units (cal/mol).

SAMPLE CASE FOR FINITE RATE CHEMISTRY

BOLT,DIL DATA								
ELT037 RLIB70 03/17-17:00:57-(,0)								
000001	000	AXQT SEAGULL						
000002	000	1	1	1	1	0	19	
000003	000	7	20	3	14	0		
000004	000	TWO DIMENSIONAL TEST CASE WITH SHOCK + INTERACTION						
000005	000	6.0	1.23	9.0	10.0	3.0		
000006	000	10.						
000007	000	10.						
000008	000	1.5						
000009	000	+20.0						
000010	000	1.0						
000011	000	10.0						
000012	000	.6805	1000.0					
000013	000	.03497	.23927	.69388	2.47	-03	.02646	2.94 -03 0.0
000014	000	H	1.008	52.102				
000015	000	200.	4.968	27.423	0.009	400.	4.968	28.852 0.506
000016	000	500.	4.968	29.961	1.003	600.	4.968	30.867 1.5
000017	000	700.	4.968	31.632	1.996	800.	4.968	32.296 2.493
000018	000	900.	4.968	32.881	2.990	1000.	4.968	33.404 3.487
000019	000	1200.	4.968	34.310	4.481	1400.	4.968	35.075 5.474
000020	000	1600.	4.968	35.739	6.468	1800.	4.968	36.325 7.461
000021	000	2000.	4.968	36.848	8.455	2200.	4.968	37.322 9.449
000022	000	2400.	4.968	37.754	10.442	2600.	4.968	38.152 11.436
000023	000	2800.	4.968	38.520	12.430	3000.	4.968	38.862 13.623
000024	000	3200.	4.968	39.183	14.417	3400.	4.968	39.484 15.410
000025	000	H2	2.016	0.0				
000026	000	200.	6.894	31.251	.013	400.	6.975	33.247 .707
000027	000	500.	6.993	34.806	1.406	600.	7.009	36.082 2.106
000028	000	700.	7.036	37.165	2.808	800.	7.087	38.107 3.514
000029	000	900.	7.148	38.946	4.226	1000.	7.219	39.702 4.944
000030	000	1200.	7.390	41.033	6.404	1400.	7.600	42.187 7.902
000031	000	1600.	7.823	43.217	9.446	1800.	8.016	44.150 11.030
000032	000	2000.	8.195	45.004	12.651	2200.	8.358	45.793 14.307
000033	000	2400.	8.506	46.527	15.993	2600.	8.639	47.213 17.708
000034	000	2800.	8.757	47.857	19.448	3000.	8.859	48.465 21.210
000035	000	3200.	8.962	49.040	22.992	3400.	9.061	49.586 24.794
000036	000	H2O	18.016	-57.798				
000037	000	200.	8.027	45.155	0.015	400.	8.186	47.484 0.825
000038	000	500.	8.415	49.334	1.654	600.	8.676	50.891 2.509
000039	000	700.	8.954	52.249	3.390	800.	9.246	53.464 4.300
000040	000	900.	9.547	54.570	5.240	1000.	9.851	55.592 6.209
000041	000	1200.	10.444	57.441	8.240	1400.	10.987	59.092 10.384
000042	000	1600.	11.462	60.591	12.630	1800.	11.869	61.965 14.964
000043	000	2000.	12.214	63.234	17.373	2200.	12.505	64.412 19.486
000044	000	2400.	12.753	65.511	22.372	2600.	12.965	66.541 24.945
000045	000	2800.	13.146	67.508	27.556	3000.	13.304	68.421 30.201
000046	000	3200.	13.441	69.284	32.876	3400.	13.562	70.102 35.577
000047	000	0	16.000	59.359				
000048	000	200.	5.235	38.501	0.010	400.	5.135	39.991 0.528
000049	000	500.	5.061	41.731	1.038	600.	5.049	42.054 1.544
000050	000	700.	5.029	42.831	2.048	800.	5.015	43.501 2.550
000051	000	900.	5.006	44.092	3.052	1000.	4.999	44.819 3.352
000052	000	1200.	4.990	45.529	4.551	1400.	4.984	46.298 5.548
000053	000	1600.	4.981	46.963	6.544	1800.	4.979	47.550 7.540
000054	000	2000.	4.978	48.074	8.536	2200.	4.979	48.549 9.532
000055	000	2400.	4.981	48.982	10.527	2600.	4.986	49.381 11.524
000056	000	2800.	4.994	49.751	12.522	3000.	5.004	50.096 13.522
000057	000	3200.	5.017	50.419	14.524	3400.	5.033	50.724 15.529

000058	000	OH	17.0074	9.432								
000059	000		200.	7.165	43.925	0.013	400.	7.087	45.974	0.725		
000060	000		500.	7.055	47.551	1.432	600.	7.057	48.837	2.137		
000061	000		700.	7.090	49.927	2.845	800.	7.150	50.877	3.556		
000062	000		900.	7.233	51.724	4.275	1000.	7.332	52.491	5.003		
000063	000		1200.	7.549	53.847	6.491	1400.	7.766	55.027	8.023		
000064	000		1600.	7.963	56.077	9.596	1800.	8.137	57.025	11.207		
000065	000		2000.	8.286	57.891	12.849	2200.	8.415	58.686	13.681		
000066	000		2400.	8.526	59.424	16.214	2600.	8.622	60.110	17.929		
000067	000		2800.	8.706	60.752	19.662	3000.	8.780	61.355	21.411		
000068	000		3200.	8.846	61.924	23.174	3400.	8.905	62.462	24.949		
000069	000		02	31.9988	0.0							
000070	000		200.	7.023	49.047	0.013	400.	7.196	51.091	0.724		
000071	000		500.	7.431	52.722	1.455	600.	7.670	54.098	2.210		
000072	000		700.	7.883	55.297	2.988	800.	8.063	56.361	3.786		
000073	000		900.	8.212	57.320	4.600	1000.	8.336	58.192	5.427		
000074	000		1200.	8.527	59.729	7.114	1400.	8.674	61.055	8.835		
000075	000		1600.	8.800	62.222	10.583	1800.	8.916	63.265	12.354		
000076	000		2000.	9.029	64.210	14.149	2200.	9.139	65.075	15.966		
000077	000		2400.	9.248	65.876	17.204	2600.	9.354	66.620	19.664		
000078	000		2800.	9.456	67.317	21.545	3000.	9.551	67.973	23.446		
000079	000		3200.	9.640	68.592	25.365	3400.	9.723	69.179	27.302		
000080	000	H ₂	33.008	E.0								
000081	000		200.	8.347	54.434	0.015	400.	8.907	56.910	0.877		
000082	000		500.	9.479	58.960	1.797	600.	9.980	60.734	2.771		
000083	000		700.	10.405	62.305	3.791	800.	10.769	63.719	4.850		
000084	000		900.	11.087	65.006	5.943	1000.	11.365	66.189	7.066		
000085	000		1200.	11.831	68.304	9.387	1400.	12.197	70.156	11.791		
000086	000		1600.	12.485	71.804	14.761	1800.	12.714	73.288	16.782		
000087	000		2000.	12.895	74.638	19.343	2200.	13.041	75.874	21.937		
000088	000		2400.	13.160	77.014	24.558	2600.	13.256	78.071	27.200		
000089	000		2800.	13.336	79.057	29.859	3000.	13.403	79.979	32.534		
000090	000		3200.0	13.50	85.0	35.0	3600.0	13.6	90.0	36.0		
000091	000	M1										
000092	000	1.0	1.0	6.0	1.0	1.0	1.0	1.0				
000093	000	M2										
000094	000	2.0	2.5	10.	1.0	1.0	1.0	1.0				
000095	000	M3										
000096	000	1.0	2.5	16.	1.0	1.0	1.0	1.0				
000097	000	H ₂ - O ₂ COMBUSTION KINETICS										
000098	000	H	+H	+M2	=H2	+M2		22	2.80-30	1.0	0.0	
000099	000	H	+0	+M1	=OH	+M1		21	1.00-32	0.0	0.2	
000100	000	H	+OH	+M1	=H2O	+M1		22	6.10-26	2.0	0.0	
000101	000	H	+O2	+M3	=HO2	+M3		23	5.5-33		1000.0	
000102	000	O	+O	+M1	=O2	+M1		24	3.80-30	1.0	-340.0	
000103	000	OH	+H		=H2	+0		14	1.40-14	-1.0	-7000.0	
000104	000	OH	+0		=H	+02		11	4.00-11	0.0	0.0	
000105	000	OH	+H2		=H2O	+H		14	1.00-17	-2.0	-2900.0	
000106	000	OH	+OH		=H2O	+0		13	1.00-11	0.0	-1100.0	
000107	000	H ₂	+H		=H2	+02		13	4.2-11		-700.0	
000108	000	H ₂	+H		=OH	+OH		13	4.2-10		-1900.0	
000109	000	H ₂	+H2		=H2O	+OH		13	1.2-12		-18700.0	
000110	000	H ₂	+O		=OH	+O2		13	8.0-11		-1000.0	
000111	000	H ₂	+OH		=H2O	+O2		13	8.3-11		-1000.0	

END ELT.

@ADD,P DATA

@XOT SEAGULL

.....
• PROGRAM SEAGULL
• SUPERSONIC INVISCID FLOW ANALYSIS
• NASA LANGLEY RESEARCH CENTER
• RELEASED 02/01/76
• LAST MODIFICATION 02/25/77
•
.....

TWO DIMENSIONAL FLOW

TWO DIMENSIONAL TEST CASE WITH SHOCK + INTERACTI
OUTPUT AT EVERY 1 STEPS

GAMMA= .1230+01 DISTANCE= .9000+01 TOLERANCE= .1000+02 SCALE
ICN=1 IBN= 1 ISO= 0 ISY= 0 ITY= 0 ITP= 0 IVI= 0
•2000+02 DEGREES BREAK IN THE UPPER WALL AT Z= .1500+01
•1000+02 DEGREES BREAK IN THE LOWER WALL AT Z= .1000+01

INITIAL CONDITIONS

TEMPERATURE (DEG. KELVIN)	1.0000000+03
VELOCITY (M/S)	5.3167825+03
PRESSURE (ATM)	6.8050000-01
DENSITY(G/CC)	1.1281265-04
MOLECULAR WT.	1.3602172+01
GAMMA	1.2846758+00
TOTAL ENTHALPY	5.7722905+11
ENTROPY	2.1301588+09
MOLE FRACTION H	3.4969999-02
MOLE FRACTION H2	2.3927000-01
MOLE FRACTION H2O	6.9387999-01
MOLE FRACTION O	2.4700000-03
MOLE FRACTION OH	2.6460000-02
MOLE FRACTION O2	2.9400000-03
MOLE FRACTION HO2	0.0000000

H2 + 32 C OMBUST ION KI NETICS

REACTIONS BEING CONSIDERED

$$K_F = A * \exp(B / RT^{**M}) / T^{**N}$$

							A	N	B	M
1	H	+ H	+ M2	= H2	+ M2		2.2	1.016+18	1.00	.00
2	H	+ O	+ M1	= OH	+ M1		2.1	3.628+15	.00	.00
3	H	+ OH	+ M1	= H2O	+ M1		2.2	2.213+22	2.00	.00
4	H	+ O2	+ M3	= HO2	+ M3		2.3	1.995+15	.00	1000.0
5	O	+ O	+ M1	= O2	+ M1		2.4	1.379+18	1.00	-340.0
6	OH	+ H		= H2	+ O		1.4	8.432+09	-1.00	-7000.0
7	OH	+ O		= H	+ O2		1.1	2.409+13	.00	.00
8	OH	+ H2		= H2O	+ H		1.4	6.023+06	-2.00	-2900.0
9	OH	+ OH		= H2O	+ O		1.3	6.023+12	.00	-1100.0
10	HO2	+ H		= H2	+ O2		1.3	2.530+13	.00	-700.0
11	HO2	+ H		= OH	+ OH		1.3	2.530+14	.00	-1900.0
12	HO2	+ H2		= H2O	+ OH		1.3	7.228+11	.00	-18700.0
13	HO2	+ O		= OH	+ O2		1.3	4.819+13	.00	-1000.0
14	HO2	+ OH		= H2O	+ O2		1.3	4.999+13	.00	-1000.0

CATALYTIC SPECIES BEING CONSIDERED

M1 = 1.00 H , 1.00 H2 , 6.00 H2O , 1.00 O , 1.00 OH , 1.00 O2 , 1.00 HO2 ,

M2 = 20.00 H , 2.50 H2 , 10.00 H2O , 1.00 O , 1.00 OH , 1.00 O2 , 1.00 HO2 ,

M3 = 1.00 H , 2.50 H2 , 16.00 H2O , 1.00 O , 1.00 OH , 1.00 O2 , 1.00 HO2 ,

K= 1 Z= .9000+00 DZ= .0000

LOWER WALL FORCES FRX=	.0000	FZ=	.0000	Mx=	.0000	VFR=	.0000	VEZ=	.0000	VM=	.0000
UPPER WALL FORCES FR=	.0000	FZ=	.0000	Mz=	.0000	VFR=	.0000	VFZ=	.0000	VM=	.0000
SUM OF FORCES	.0000		.0000		.0000		.0000		.0000		.0000
FORCE ON COMPUTATIONAL PLANE=	.0000	AREA=	.0000								
MOMENT ABOUT R AXIS=	.0000	MOMENT ABOUT Z AXIS=	.0000								

I	N	R	P	U	W	T	S	M	THE	RHO	HTOT
0	21	.1000+01	.1000+01	.0000	.6801+01	.1000+01	.0000	.6000+01	.0000	.1000+01	.1538+01
C	20	.9474+00	.1000+01	.0000	.6801+01	.1000+01	.0000	.6000+01	.0000	.1000+01	.1538+01
0	19	.8947+00	.1000+01	.0000	.6801+01	.1000+01	.0000	.6000+01	.0000	.1000+01	.1538+01
0	18	.8421+00	.1000+01	.0000	.6801+01	.1000+01	.0000	.6000+01	.0000	.1000+01	.1538+01
C	17	.7895+00	.1000+01	.0000	.6801+01	.1000+01	.0000	.6000+01	.0000	.1000+01	.1538+01
0	16	.7368+00	.1000+01	.0000	.6801+01	.1000+01	.0000	.5000+01	.0000	.1000+01	.1538+01
0	15	.6842+00	.1000+01	.0000	.6801+01	.1000+01	.0000	.6000+01	.0000	.1000+01	.1538+01
C	14	.6316+00	.1000+01	.0000	.6801+01	.1000+01	.0000	.6000+01	.0000	.1000+01	.1538+01
0	13	.5789+00	.1000+01	.0000	.6801+01	.1000+01	.0000	.6000+01	.0000	.1000+01	.1538+01
C	12	.5263+00	.1000+01	.0000	.6801+01	.1000+01	.0000	.6000+01	.0000	.1000+01	.1538+01
C	11	.4737+00	.1000+01	.0000	.6801+01	.1000+01	.0000	.6000+01	.0000	.1000+01	.1538+01
C	10	.4211+00	.1000+01	.0000	.6801+01	.1000+01	.0000	.6000+01	.0000	.1000+01	.1538+01
0	9	.3684+00	.1000+01	.0000	.6801+01	.1000+01	.0000	.6000+01	.0000	.1000+01	.1538+01

0	8	.3158+00	.1000+01	.0000	.6801+01	.1000+01	.0000	.6000+01	.0000	.1000+01	.1538+01
0	7	.2632+00	.1000+01	.0000	.6801+01	.1000+01	.0000	.6000+01	.0000	.1000+01	.1538+01
0	6	.2105+00	.1000+01	.0000	.6801+01	.1000+01	.0000	.6000+01	.0000	.1000+01	.1538+01
0	5	.1579+00	.1000+01	.0000	.6801+01	.1000+01	.0000	.6000+01	.0000	.1000+01	.1538+01
0	4	.1053+00	.1000+01	.0000	.6801+01	.1000+01	.0000	.6000+01	.0000	.1000+01	.1538+01
0	3	.5263-01	.1000+01	.0000	.6801+01	.1000+01	.0000	.6000+01	.0000	.1000+01	.1538+01
0	-2	.0000	.1000+01	.0000	.6801+01	.1000+01	.0000	.6000+01	.0000	.1000+01	.1538+01

MOLE FRACTIONS

PT	R(N)	H	H2	H2O	O	OH	O2	H2O2	MOL WT	GAMMA
21	1.00000	3.49704-02	2.39272-01	6.93887-01	2.47002-03	2.64603-02	2.94003-03	0.00000	9.99990-01	1.28467+00
20	.94737	3.49704-02	2.39272-01	6.93887-01	2.47002-03	2.64603-02	2.94003-03	0.00000	9.99990-01	1.28467+00
19	.89474	3.49704-02	2.39272-01	6.93887-01	2.47002-03	2.64603-02	2.94003-03	0.00000	9.99990-01	1.28467+00
18	.84211	3.49704-02	2.39272-01	6.93887-01	2.47002-03	2.64603-02	2.94003-03	0.00000	9.99990-01	1.28467+00
17	.78947	3.49704-02	2.39272-01	6.93887-01	2.47002-03	2.64603-02	2.94003-03	0.00000	9.99990-01	1.28467+00
16	.73684	3.49704-02	2.39272-01	6.93887-01	2.47002-03	2.64603-02	2.94003-03	0.00000	9.99990-01	1.28467+00
15	.68421	3.49704-02	2.39272-01	6.93887-01	2.47002-03	2.64603-02	2.94003-03	0.00000	9.99990-01	1.28467+00
14	.63158	3.49704-02	2.39272-01	6.93887-01	2.47002-03	2.64603-02	2.94003-03	0.00000	9.99990-01	1.28467+00
13	.57895	3.49704-02	2.39272-01	6.93887-01	2.47002-03	2.64603-02	2.94003-03	0.00000	9.99990-01	1.28467+00
12	.52632	3.49704-02	2.39272-01	6.93887-01	2.47002-03	2.64603-02	2.94003-03	0.00000	9.99990-01	1.28467+00
11	.47368	3.49704-02	2.39272-01	6.93887-01	2.47002-03	2.64603-02	2.94003-03	0.00000	9.99990-01	1.28467+00
10	.42105	3.49704-02	2.39272-01	6.93887-01	2.47002-03	2.64603-02	2.94003-03	0.00000	9.99990-01	1.28467+00
9	.36842	3.49704-02	2.39272-01	6.93887-01	2.47002-03	2.64603-02	2.94003-03	0.00000	9.99990-01	1.28467+00
8	.31579	3.49704-02	2.39272-01	6.93887-01	2.47002-03	2.64603-02	2.94003-03	0.00000	9.99990-01	1.28467+00
7	.26316	3.49704-02	2.39272-01	6.93887-01	2.47002-03	2.64603-02	2.94003-03	0.00000	9.99990-01	1.28467+00
6	.21053	3.49704-02	2.39272-01	6.93887-01	2.47002-03	2.64603-02	2.94003-03	0.00000	9.99990-01	1.28467+00
5	.15789	3.49704-02	2.39272-01	6.93887-01	2.47002-03	2.64603-02	2.94003-03	0.00000	9.99990-01	1.28467+00
4	.10526	3.49704-02	2.39272-01	6.93887-01	2.47002-03	2.64603-02	2.94003-03	0.00000	9.99990-01	1.28467+00
3	.05263	3.49704-02	2.39272-01	6.93887-01	2.47002-03	2.64603-02	2.94003-03	0.00000	9.99990-01	1.28467+00
2	.00000	3.49704-02	2.39272-01	6.93887-01	2.47002-03	2.64603-02	2.94003-03	0.00000	9.99990-01	1.28467+00

SAMPLE CASE FOR VIBRATIONAL NON-EQUILIBRIUM

@ELT,DIL DATA
 ELT007 RLIB70 12/01-19:12:01-(,0)
 000001 000 @XQT SEAGULL
 000002 000 1 100 1 1 -0 .19
 000003 000 12 24 4 26 0
 000004 000 CCCC UUJO CASE ***
 000005 000 4.u 1.e 430.0 10.0 3.u
 000006 000 434.
 000007 000 434.
 000008 000 1.0
 000009 000 -30.0
 000010 000 C.998
 000011 000 -3u.
 000012 000 2.0 2000. 4340.
 000013 000 0.00322 0.00162 0.00876 0.01083 0.01018 0.00873 0.00393
 000014 000 0.37433 0.07024 0.05909 0.02363 0.42544
 000015 000 C02100 44.01 -90.081
 000016 000 0. 6.955 37.932 -2.074 50. 6.955 37.932 -1.725
 000017 000 100. 6.955 42.753 -1.378 150. 6.955 45.574 -1.030
 000018 000 200. 6.955 47.575 -0.682 250. 6.955 49.127 -0.334
 000019 000 300. 6.955 50.395 0.013 400. 6.955 52.396 0.709
 000020 000 500. 6.955 53.948 1.404 600. 6.955 55.216 2.100
 000021 000 700. 6.955 56.288 2.796 800. 6.955 57.217 3.491
 000022 000 900. 6.955 58.036 4.187 1000. 6.955 58.769 4.882
 000023 000 1200. 6.955 60.037 6.273 1400. 6.955 61.109 7.664
 000024 000 1600. 6.955 62.038 9.055 1800. 6.955 62.857 10.446
 000025 000 2000. 6.955 63.590 11.838 2200. 6.955 64.253 13.229
 000026 000 2400. 6.955 64.858 14.620 2600. 6.955 65.415 16.011
 000027 000 2800. 6.955 65.930 17.402 3000. 6.955 66.410 18.793
 000028 000 C02001 44.01 -87.331
 000029 000 0. 6.955 37.932 -2.074 50. 6.955 37.932 -1.725
 000030 000 100. 6.955 42.753 -1.378 150. 6.955 45.574 -1.030
 000031 000 200. 6.955 47.575 -0.682 250. 6.955 49.127 -0.334
 000032 000 300. 6.955 50.395 0.013 400. 6.955 52.396 0.709
 000033 000 500. 6.955 53.948 1.404 600. 6.955 55.216 2.100
 000034 000 700. 6.955 56.288 2.796 800. 6.955 57.217 3.491
 000035 000 900. 6.955 58.036 4.187 1000. 6.955 58.769 4.882
 000036 000 1200. 6.955 60.037 6.273 1400. 6.955 61.109 7.664
 000037 000 1600. 6.955 62.038 9.055 1800. 6.955 62.857 10.446
 000038 000 2000. 6.955 63.590 11.838 2200. 6.955 64.253 13.229
 000039 000 2400. 6.955 64.858 14.620 2600. 6.955 65.415 16.011
 000040 000 2800. 6.955 65.930 17.402 3000. 6.955 66.410 18.793
 000041 000 C02000 44.01 -94.051

000042	000	0.	6.955	37.932	-2.074	50.	6.955	37.932	-1.725
000043	000	100.	6.955	42.753	-1.378	150.	6.955	45.574	-1.030
000044	000	200.	6.955	47.575	-0.682	250.	6.955	49.127	-0.334
000045	000	300.	6.955	50.395	0.013	400.	6.955	52.396	0.709
000046	000	500.	6.955	53.948	1.404	600.	6.955	55.216	2.100
000047	000	700.	6.955	56.288	2.796	800.	6.955	57.217	3.491
000048	000	900.	6.955	58.036	4.187	1000.	6.955	58.769	4.882
000049	000	1200.	6.955	60.037	6.273	1400.	6.955	61.109	7.664
000050	000	1600.	6.955	62.038	9.055	1800.	6.955	62.857	10.446
000051	000	2000.	6.955	63.590	11.838	2200.	6.955	64.253	13.229
000052	000	2400.	6.955	64.856	14.620	2600.	6.955	65.415	16.011
000053	000	2800.	6.955	65.930	17.402	3000.	6.955	66.410	18.793
000054	000	C02110 44.01	-88.111						
000055	000	0.	6.955	39.31	-2.074	50.	6.955	39.31	-1.725
000056	000	100.	6.955	44.131	-1.378	150.	6.955	46.951	-1.030
000057	000	200.	6.955	48.952	-0.682	250.	6.955	50.504	-0.334
000058	000	300.	6.955	51.772	0.013	400.	6.955	53.773	0.709
000059	000	500.	6.955	55.325	1.404	600.	6.955	56.593	2.100
000060	000	700.	6.955	57.665	2.796	800.	6.955	58.594	3.491
000061	000	900.	6.955	59.413	4.187	1000.	6.955	60.146	4.882
000062	000	1200.	6.955	61.414	6.273	1400.	6.955	62.487	7.664
000063	000	1600.	6.955	63.415	9.055	1800.	6.955	64.235	10.446
000064	000	2000.	6.955	64.967	11.838	2200.	6.955	65.63	13.229
000065	000	2400.	6.955	66.235	14.620	2600.	6.955	66.792	16.011
000066	000	2800.	6.955	67.308	17.402	3000.	6.955	67.788	18.793
000067	000	C02010 44.01	-92.141						
000068	000	0.	6.955	39.31	-2.074	50.	6.955	39.31	-1.725
000069	000	100.	6.955	44.131	-1.378	150.	6.955	46.951	-1.030
000070	000	200.	6.955	48.952	-0.682	250.	6.955	50.504	-0.334
000071	000	300.	6.955	51.772	0.013	400.	6.955	53.773	0.709
000072	000	500.	6.955	55.325	1.404	600.	6.955	56.593	2.100
000073	000	700.	6.955	57.665	2.796	800.	6.955	58.594	3.491
000074	000	900.	6.955	59.413	4.187	1000.	6.955	60.146	4.882
000075	000	1200.	6.955	61.414	6.273	1400.	6.955	62.487	7.664
000076	000	1600.	6.955	63.415	9.055	1800.	6.955	64.235	10.446
000077	000	2000.	6.955	64.967	11.838	2200.	6.955	65.63	13.229
000078	000	2400.	6.955	66.235	14.620	2600.	6.955	66.792	16.011
000079	000	2800.	6.955	67.308	17.402	3000.	6.955	67.788	18.793
000080	000	C02020 44.01	-99.284						
000081	000	0.	6.955	40.115	-2.074	50.	6.955	40.115	-1.725
000082	000	100.	6.955	44.936	-1.378	150.	6.955	47.757	-1.030
000083	000	200.	6.955	49.758	-0.682	250.	6.955	51.310	-0.334
000084	000	300.	6.955	52.578	0.013	400.	6.955	54.579	0.709
000085	000	500.	6.955	56.131	1.404	600.	6.955	57.399	2.100
000086	000	700.	6.955	58.471	2.796	800.	6.955	59.400	3.491
000087	000	900.	6.955	60.219	4.187	1000.	6.955	60.952	4.882
000088	000	1200.	6.955	62.220	6.273	1400.	6.955	63.292	7.664
000089	000	1600.	6.955	64.221	9.055	1800.	6.955	64.040	10.446
000090	000	2000.	6.955	65.773	11.838	2200.	6.955	66.436	13.229
000091	000	2400.	6.955	66.041	14.620	2600.	6.955	67.598	16.011
000092	000	2800.	6.955	68.113	17.402	3000.	6.955	68.593	18.793
000093	000	C02030 44.01	-88.531						

000094	000	0.	6.955	40.687	-2.074	50.	6.955	40.687	-1.725
000095	000	100.	6.955	45.508	-1.378	150.	6.955	48.329	-1.030
000096	000	200.	6.955	50.329	-0.682	250.	6.955	51.882	-0.334
000097	000	300.	6.955	53.150	0.013	400.	6.955	55.151	0.709
000098	000	500.	6.955	56.703	1.404	600.	6.955	57.971	2.100
000099	000	700.	6.955	59.043	2.796	800.	6.955	59.972	3.491
000100	000	900.	6.955	60.791	4.187	1000.	6.955	61.524	4.882
000101	000	1200.	6.955	62.792	6.273	1400.	6.955	63.664	7.664
000102	000	1600.	6.955	64.793	9.055	1800.	6.955	65.612	10.446
000103	000	2000.	6.955	66.345	11.838	2200.	6.955	67.008	13.229
000104	000	2400.	6.955	67.613	14.620	2600.	6.955	68.170	16.011
000105	000	2800.	6.955	68.685	17.402	3000.	6.955	69.165	18.793
000106	000	N2(0)	28.016	0.0	3.798	71.4			
000107	000	0.	6.955	33.339	-2.075	50.	6.955	33.339	-1.727
000108	000	100.	6.956	38.160	-1.379	150.	6.956	40.981	-1.031
000109	000	200.	6.957	42.982	-0.683	250.	6.957	44.535	-0.335
000110	000	300.	6.958	45.803	0.013	400.	6.959	47.805	0.709
000111	000	500.	6.960	49.357	1.405	600.	6.962	50.627	2.101
000112	000	700.	6.965	51.700	2.797	800.	6.968	52.631	3.494
000113	000	900.	6.972	53.451	4.190	1000.	6.975	54.186	4.888
000114	000	1200.	6.983	55.458	6.284	1400.	6.991	56.535	7.681
000115	000	1600.	6.999	57.470	8.963	1800.	7.008	58.294	10.481
000116	000	2000.	7.015	59.033	11.883	2200.	7.022	59.702	13.287
000117	000	2400.	7.031	60.313	14.692	2600.	7.038	60.876	16.099
000118	000	2800.	7.045	61.399	17.507	3000.	7.052	61.885	18.917
000119	000	N2(1)	28.016	6.655	3.798	71.4			
000120	000	0.	6.955	33.339	-2.075	50.	6.955	33.339	-1.727
000121	000	100.	6.956	38.160	-1.379	150.	6.956	40.981	-1.031
000122	000	200.	6.957	42.982	-0.683	250.	6.957	44.535	-0.335
000123	000	300.	6.958	45.803	0.013	400.	6.959	47.805	0.709
000124	000	500.	6.960	49.357	1.405	600.	6.962	50.627	2.101
000125	000	700.	6.965	51.700	2.797	800.	6.968	52.631	3.494
000126	000	900.	6.972	53.451	4.190	1000.	6.975	54.186	4.888
000127	000	1200.	6.983	55.458	6.284	1400.	6.991	56.535	7.681
000128	000	1600.	6.999	57.470	8.963	1800.	7.008	58.294	10.481
000129	000	2000.	7.015	59.033	11.883	2200.	7.022	59.702	13.287
000130	000	2400.	7.031	60.313	14.692	2600.	7.038	60.876	16.099
000131	000	2800.	7.045	61.399	17.507	3000.	7.052	61.885	18.917
000132	000	02	31.9988	0.0					
000133	000	0.	6.958	36.572	-2.075	50.	6.958	36.572	-1.729
000134	000	100.	6.958	41.395	-1.381	150.	6.960	44.216	-1.033
000135	000	200.	6.961	46.218	-0.685	250.	6.992	47.769	-0.337
000136	000	300.	7.023	49.047	0.013	400.	7.196	51.091	0.724
000137	000	500.	7.431	52.722	1.455	600.	7.670	54.098	2.210
000138	000	700.	7.883	55.297	2.988	800.	8.063	56.361	3.786
000139	000	900.	8.212	57.320	4.600	1000.	8.336	58.192	5.427
000140	000	1200.	8.527	59.729	7.114	1400.	9.674	61.055	8.835
000141	000	1600.	8.900	62.222	10.583	1800.	8.916	63.265	12.354
000142	000	2000.	9.029	64.210	14.149	2200.	9.139	65.076	15.966
000143	000	2400.	9.248	65.876	17.804	2600.	9.354	66.620	19.664
000144	000	2800.	9.455	67.317	21.545	3000.	9.551	67.973	23.446
000145	000	H2O	18.016	-57.798					

000146	000	0.0	0.0	0.0	-2.367	50.	3.9805	18.198	-1.974
000147	000	100.	7.961	36.396	-1.581	150.	7.965	39.156	-1.18
000148	000	200.	7.969	41.916	- .784	250.	7.998	43.535	- .384
000149	000	300.	8.027	45.155	.015	400.	8.186	47.483	.825
000150	000	500.	8.415	49.334	1.654	600.	8.676	50.891	2.509
000151	000	700.	8.954	52.249	3.390	800.	9.246	53.464	4.300
000152	000	900.0	9.547	54.570	5.240	1000.0	9.851	55.591	6.209
000153	000	1200.0	10.444	57.440	8.240	1400.0	10.987	59.092	10.384
000154	000	1600.0	11.462	60.591	12.630	1800.0	11.869	61.965	14.964
000155	000	2000.0	12.214	63.234	17.373	2200.0	12.505	64.412	19.846
000156	000	2400.0	12.753	65.511	22.372	2600.0	12.965	66.540	24.945
000157	000	2800.0	13.146	67.508	27.556	3000.0	13.304	68.420	30.201
000158	000	HE	4.003	0.					
000159	000	0.	4.968	21.255	-1.481	50.	4.968	21.255	-1.233
000160	000	100.	4.968	24.698	-0.984	150.	4.968	26.128	-0.736
000161	000	200.	4.968	28.142	-0.488	250.	4.968	29.048	-0.239
000162	000	300.	4.968	30.156	0.009	400.	4.968	31.586	0.506
000163	000	500.	4.968	32.694	1.003	600.	4.968	33.600	1.500
000164	000	700.	4.968	34.366	1.996	800.	4.968	35.029	2.493
000165	000	900.	4.968	35.614	2.990	1000.	4.968	36.138	3.487
000166	000	1200.	4.968	37.044	4.481	1400.	4.968	37.809	5.474
000167	000	1600.	4.968	38.473	6.468	1800.	4.968	39.058	7.461
000168	000	2000.	4.968	39.581	8.455	2200.	4.968	40.055	9.449
000169	000	2400.	4.968	40.487	10.442	2600.	4.968	40.885	11.436
000170	000	2800.	4.968	41.253	12.430	3000.	4.968	41.596	13.423
000171	000	M1							
000172	000	1.0	1.0	1.0	1.0	1.0	0.0	0.0	1.0
000173	000	M2							
000174	000	1.0	1.0	1.0	1.0	1.0	1.0	1.0	1.0
000175	000	M3							
000176	000	1.0	1.0	1.0	1.0	1.0	0.5	0.5	1.0
000177	000	M4							
000178	000	0.0	0.0	0.0	0.0	0.0	2.0	2.0	0.0
000179	000	C02 GDL REACTION MODEL (AIR-BREATHING)					19 OCT 1976	26 REACTIONS	
000180	000	C02110+C02000		=C02100+C02010			12	1.25-13-0.5	
000181	000	C02030+C02000		=C02100+C02010			12	1.8 -15-0.5	
000182	000	C02030+C02000		=C02020+C02010			12	3.1 -13-0.5	
000183	000	C02100+C02000		=C02010+C02010			11	4.0 -13	
000184	000	C02020+C02000		=C02010+C02010			12	1.4 -12-0.5	
000185	000	C02001+M1		=C02110+M1			64	1.1 -27-4.8	1484.
000186	000	C02001+M4		=C02110+M4			64	1.9 -31-5.8	2436.
000187	000	C02001+M1		=C02030+M1			64	8.1 -31-5.6	1484.
000188	000	C02001+M4		=C02030+M4			64	1.4 -34-6.6	2436.
000189	000	C02110+M2		=C02030+M2			62	4.3 -17-1.5	
000190	000	C02110+M2		=C02020+M2			64	4.5 -27-4.2	- 903.

000191	000	C02110+M2	=C02020+M2	64 8.8 -20-2.5 - 4410.
000192	000	C02110+M2	=C02100+M2	64 8.6 -24-3.8 - 549.
000193	000	C02030+M2	=C02020+M2	64 9.3 -22-3.3 - 1230.
000194	000	C02030+M2	=C02100+M2	64 1.1 -21-3.0 - 1060.
000195	000	C02100+M2	=C02020+M2	62 8.0 -18-1.5
000196	000	C02100+M3	=C02010+M3	64 5.6 -22-3.3 - 1480.
000197	000	C02100+HE	=C02010+HE	14 1.8 -21-3.0 843.
000198	000	C02020+M3	=C02010+M3	64 2.1 -21-3.2 - 1350.
000199	000	C02020+HE	=C02010+HE	14 3.8 -21-3.0 843.
000200	000	C02010+M3	=C02000+M3	64 3.4 -26-4.2 1150.
000201	000	C02010+HE	=C02000+HE	14 9.9 -22-3.0 843.
000202	000	C02001+N2(0)	=C02000+N2(1)	12 8.3 -12 0.5
000203	000	C02010+H2O	=C02000+H2O	15 3.2 -13 45.5 0.333
000204	000	C02001+H2O	=C02030+H2O	11 4.0 -13
000205	000	N2(1) +H2O	=N2(0) +H2O	15 1.1 -10 - 139.0 0.333

END ELT.

@ADD,P DATA

@XQT SEAGULL

• PROGRAM SEAGULL
• SUPERSONIC INVISCID FLOW ANALYSIS
• NASA Langley Research Center
• RELEASED 02/01/76
• LAST MODIFICATION 02/25/77
•

TWO DIMENSIONAL FLOW
CCCC 0000 C A S E ***
OUTPUT AT EVERY 100 STEPS
GAMMA= .1200+01 DISTANCE= .4300+03 TOLERANCE= .1000+02 SCALE= .3000+01
ICN= 1 IBN= 1 ISO= 0 ISY= 0 ITY= 0 ITP= 0 IVI= 0
-.3000+02 DEGREES BREAK IN THE UPPER WALL AT Z= .1000+01
-.3000+02 DEGREES BREAK IN THE LOWER WALL AT Z= .9980+00

INITIAL CONDITIONS

TEMPERATURE(DEG. KELVIN)	2.0000000+03
VELOCITY (M/S)	4.5628436+03
PRESSURE(ATM)	2.0000000+00
DENSITY(G/CC)	2.2614246-04
MOLECULAR WT.	1.8554989+01
GAMMA	1.4520176+00
TOTAL ENTHALPY	2.1616025+12
ENTROPY	2.1521133+09
MOLE FRACTION C02100	3.2200000-03
MOLE FRACTION C02001	1.6200000-03
MOLE FRACTION C02000	8.7599999-03
MOLE FRACTION C02110	1.0830000-02
MOLE FRACTION C02010	1.0180000-02
MOLE FRACTION C02020	8.7299999-03
MOLE FRACTION C02030	3.9299999-03
MOLE FRACTION N2(0)	3.7432999-01
MOLE FRACTION N2(1)	7.0239999-02
MOLE FRACTION O2	5.9090000-02
MOLE FRACTION H2O	2.3630000-02
MOLE FRACTION HE	4.2543999-01

C02 G DL REA CTION MODEL (AIR-B REATHI NG) 1
 REACTIONS BEING CONSIDERED

					A	N	B	M
1	C02110+ C02000	= C02100+ C02010	1 2	7.529+10	-.50	.0	.00	
2	C02030+ C02000	= C02100+ C02010	1 2	1.084+09	-.50	.0	.00	
3	C02030+ C02000	= C02020+ C02010	1 2	1.867+11	-.50	.0	.00	
4	C02100+ C02000	= C02010+ C02013	1 1	2.409+11	.00	.0	.00	
5	C02020+ C02000	= C02010+ C02010	1 2	8.432+11	-.50	.0	.00	
6	C02001+ M1	= C02110+ M1	6 4	6.626+04	-4.80	1484.0	.00	
7	C02001+ M4	= C02110+ M4	6 4	1.144+07	-5.80	2436.0	.00	
8	C02001+ M1	= C02030+ M1	6 4	4.879+07	-5.60	1484.0	.00	
9	C02001+ M4	= C02030+ M4	6 4	8.432+11	-6.60	2436.0	.00	
10	C02110+ M2	= C02030+ M2	6 2	2.590+07	-1.50	.0	.00	
11	C02110+ M2	= C02020+ M2	6 4	2.710+03	-4.20	-903.0	.00	
12	C02110+ M2	= C02020+ M2	6 4	5.300+04	-2.50	-4410.0	.00	
13	C02110+ M2	= C02100+ M2	6 4	5.180+00	-3.80	-549.0	.00	
14	C02030+ M2	= C02020+ M2	6 4	5.602+02	-3.30	-1230.0	.00	
15	C02030+ M2	= C02100+ M2	6 4	6.626+02	-3.00	-1060.0	.00	
16	C02100+ M2	= C02020+ M2	6 2	4.819+06	-1.50	.0	.00	
17	C02100+ M3	= C02010+ M3	6 4	3.373+02	-3.30	-1480.0	.00	
18	C02100+ HE	= C02010+ HE	1 4	1.084+03	-3.00	843.0	.00	
19	C02020+ M3	= C02010+ M3	6 4	1.265+03	-3.20	-1350.0	.00	
20	C02020+ HE	= C02010+ HE	1 4	2.289+03	-3.00	843.0	.00	
21	C02010+ M3	= C02000+ M3	6 4	2.048+02	-4.20	1130.0	.00	
22	C02010+ HE	= C02000+ HE	1 4	5.963+02	-3.00	843.0	.00	
23	C02001+ N2(0)	= C02000+ N2(1)	1 2	4.999+12	.50	.0	.00	
24	C02010+ H2O	= C02000+ H2O	1 5	1.927+11	.00	45.5	.33	
25	C02001+ H2O	= C02030+ H2O	1 1	2.409+11	.00	.0	.00	
26	N2(1) + H2O	= N2(0) + H2O	1 5	6.626+13	.00	-139.0	.33	

CATALYTIC SPECIES BEING CONSIDERED

M1 = 1.00 C02100, 1.00 C02001, 1.00 C02000, 1.00 C02110, 1.00 C02010, 1.00 C02020, 1.00 C02030,
 .00 N2(0) , .00 N2(1) , .00 02 , 1.00 H2O , .00 HE ,
 M2 = 1.00 C02100, 1.00 C02001, 1.00 C02000, 1.00 C02110, 1.00 C02010, 1.00 C02020, 1.00 C02030,
 1.00 N2(0) , 1.00 N2(1) , 1.00 02 , 1.00 H2O , 1.50 HE ,
 M3 = 1.00 C02100, 1.00 C02001, 1.00 C02000, 1.00 C02110, 1.00 C02010, 1.00 C02020, 1.00 C02030,
 .50 N2(0) , .50 N2(1) , .60 02 , 1.00 H2O , .00 HE ,
 M4 = .00 C02100, .00 C02001, .00 C02000, .00 C02110, .00 C02010, .00 C02020, .00 C02030,
 2.00 N2(0) , 2.00 N2(1) , 2.40 02 , .00 H2O , 1.00 HE ,

K= 0 Z= .9950+00 DZ= .0000

LOWER WALL FORCES FR= .0000 FZ= .0000 M= .0000 VFR= .0000 VFZ= .0000 VM= .0000
 UPPER WALL FORCES FR= .0000 FZ= .0000 M= .0000 VFR= .0000 VFZ= .0000 VM= .0000
 SUM OF FORCES .0000 .0000 .0000 .0000 .0000 .0000 .0000 .0000
 FORCE ON COMPUTATIONAL PLANE= .0000 AREA= .0000
 MOMENT ABOUT R AXIS= .0000 MOMENT ABOUT Z AXIS= .0000

I	N	R	P	U	V	T	S	M	THE	RHO	HTOT
0	21	.1100+03	.1000+01	.0000	.4820+01	.1000+01	.0000	.4000+01	.0000	.1000+01	.4047+01
0	20	.1095+03	.1000+01	.0000	.4820+01	.1000+01	.0000	.4000+01	.0000	.1000+01	.4047+01
0	19	.1089+03	.1000+01	.0000	.4820+01	.1000+01	.0000	.4000+01	.0000	.1000+01	.4047+01
0	18	.1084+03	.1000+01	.0000	.4820+01	.1000+01	.0000	.4000+01	.0000	.1000+01	.4047+01
0	17	.1079+03	.1000+01	.0000	.4820+01	.1000+01	.0000	.4000+01	.0000	.1000+01	.4047+01
0	16	.1074+03	.1000+01	.0000	.4820+01	.1000+01	.0000	.4000+01	.0000	.1000+01	.4047+01
0	15	.1068+03	.1000+01	.0000	.4820+01	.1000+01	.0000	.4000+01	.0000	.1000+01	.4047+01
0	14	.1063+03	.1000+01	.0000	.4820+01	.1000+01	.0000	.4000+01	.0000	.1000+01	.4047+01
0	13	.1058+03	.1000+01	.0000	.4820+01	.1000+01	.0000	.4000+01	.0000	.1000+01	.4047+01
0	12	.1053+03	.1000+01	.0000	.4820+01	.1000+01	.0000	.4000+01	.0000	.1000+01	.4047+01
0	11	.1047+03	.1000+01	.0000	.4820+01	.1000+01	.0000	.4000+01	.0000	.1000+01	.4047+01
0	10	.1042+03	.1000+01	.0000	.4820+01	.1000+01	.0000	.4000+01	.0000	.1000+01	.4047+01
0	9	.1037+03	.1000+01	.0000	.4820+01	.1000+01	.0000	.4000+01	.0000	.1000+01	.4047+01
0	8	.1032+03	.1000+01	.0000	.4820+01	.1000+01	.0000	.4000+01	.0000	.1000+01	.4047+01
0	7	.1026+03	.1000+01	.0000	.4820+01	.1000+01	.0000	.4000+01	.0000	.1000+01	.4047+01
0	6	.1021+03	.1000+01	.0000	.4820+01	.1000+01	.0000	.4000+01	.0000	.1000+01	.4047+01
0	5	.1016+03	.1000+01	.0000	.4820+01	.1000+01	.0000	.4000+01	.0000	.1000+01	.4047+01
0	4	.1011+03	.1000+01	.0000	.4820+01	.1000+01	.0000	.4000+01	.0000	.1000+01	.4047+01
0	3	.1005+03	.1000+01	.0000	.4820+01	.1000+01	.0000	.4000+01	.0000	.1000+01	.4047+01
0	2	.1000+03	.1000+01	.0000	.4820+01	.1000+01	.0000	.4000+01	.0000	.1000+01	.4047+01

MOLE FRACTIONS

PT	R(IN)	C02100	C02001	C02000	C02110	C02010	C02020	C02030	MOL WT	GAMMA
2110.00000	3.22000-03	1.62000-03	8.76000-03	1.08300-02	1.01800-02	8.73000-03	3.93000-03	1.00000+00	1.45202+00	
20109.47368	3.22000-03	1.62000-03	8.76000-03	1.08300-02	1.01800-02	8.73000-03	3.93000-03	1.00000+00	1.45202+00	
19108.94737	3.22000-03	1.62000-03	8.76000-03	1.08300-02	1.01800-02	8.73000-03	3.93000-03	1.00000+00	1.45202+00	
18108.42105	3.22000-03	1.62000-03	8.76000-03	1.08300-02	1.01800-02	8.73000-03	3.93000-03	1.00000+00	1.45202+00	
17107.89474	3.22000-03	1.62000-03	8.76000-03	1.08300-02	1.01800-02	8.73000-03	3.93000-03	1.00000+00	1.45202+00	
16107.36842	3.22000-03	1.62000-03	8.76000-03	1.08300-02	1.01800-02	8.73000-03	3.93000-03	1.00000+00	1.45202+00	
15106.84210	3.22000-03	1.62000-03	8.76000-03	1.08300-02	1.01800-02	8.73000-03	3.93000-03	1.00000+00	1.45202+00	
14106.31579	3.22000-03	1.62000-03	8.76000-03	1.08300-02	1.01800-02	8.73000-03	3.93000-03	1.00000+00	1.45202+00	
13105.78947	3.22000-03	1.62000-03	8.76000-03	1.08300-02	1.01800-02	8.73000-03	3.93000-03	1.00000+00	1.45202+00	
12105.26316	3.22000-03	1.62000-03	8.76000-03	1.08300-02	1.01800-02	8.73000-03	3.93000-03	1.00000+00	1.45202+00	
11154.73684	3.22000-03	1.62000-03	8.76000-03	1.08300-02	1.01800-02	8.73000-03	3.93000-03	1.00000+00	1.45202+00	
10104.21053	3.22000-03	1.62000-03	8.76000-03	1.08300-02	1.01800-02	8.73000-03	3.93000-03	1.00000+00	1.45202+00	
9103.68421	3.22000-03	1.62000-03	8.76000-03	1.08300-02	1.01800-02	8.73000-03	3.93000-03	1.00000+00	1.45202+00	
8103.15789	3.22000-03	1.62000-03	8.76000-03	1.08300-02	1.01800-02	8.73000-03	3.93000-03	1.00000+00	1.45202+00	
7102.63158	3.22000-03	1.62000-03	8.76000-03	1.08300-02	1.01800-02	8.73000-03	3.93000-03	1.00000+00	1.45202+00	
6102.10526	3.22000-03	1.62000-03	8.76000-03	1.08300-02	1.01800-02	8.73000-03	3.93000-03	1.00000+00	1.45202+00	
5101.57895	3.22000-03	1.62000-03	8.76000-03	1.08300-02	1.01800-02	8.73000-03	3.93000-03	1.00000+00	1.45202+00	
4101.05263	3.22000-03	1.62000-03	8.76000-03	1.08300-02	1.01800-02	8.73000-03	3.93000-03	1.00000+00	1.45202+00	
3100.52632	3.22000-03	1.62000-03	8.76000-03	1.08300-02	1.01800-02	8.73000-03	3.93000-03	1.00000+00	1.45202+00	
2100.00000	3.22000-03	1.62000-03	8.76000-03	1.08300-02	1.01800-02	8.73000-03	3.93000-03	1.00000+00	1.45202+00	

MOLE FRACTIONS

PT	R(N)	N2(0)	N2(1)	O2	H2O	HE	
21110.00000	3.74330-01	7.02400-02	5.90900-02	2.36300-02	4.25440-01	1.00000+00	1.45202+00
20109.47368	3.74330-01	7.02400-02	5.90900-02	2.36300-02	4.25440-01	1.00000+00	1.45202+00
19108.94737	3.74330-01	7.02400-02	5.90900-02	2.36300-02	4.25440-01	1.00000+00	1.45202+00
18108.42105	3.74330-01	7.02400-02	5.90900-02	2.36300-02	4.25440-01	1.00000+00	1.45202+00
17107.89474	3.74330-01	7.02400-02	5.90900-02	2.36300-02	4.25440-01	1.00000+00	1.45202+00
16107.36842	3.74330-01	7.02400-02	5.90900-02	2.36300-02	4.25440-01	1.00000+00	1.45202+00
15106.84210	3.74330-01	7.02400-02	5.90900-02	2.36300-02	4.25440-01	1.00000+00	1.45202+00
14106.31579	3.74330-01	7.02400-02	5.90900-02	2.36300-02	4.25440-01	1.00000+00	1.45202+00
13105.78947	3.74330-01	7.02400-02	5.90900-02	2.36300-02	4.25440-01	1.00000+00	1.45202+00
12105.26316	3.74330-01	7.02400-02	5.90900-02	2.36300-02	4.25440-01	1.00000+00	1.45202+00
11104.73684	3.74330-01	7.02400-02	5.90900-02	2.36300-02	4.25440-01	1.00000+00	1.45202+00
10104.21053	3.74330-01	7.02400-02	5.90900-02	2.36300-02	4.25440-01	1.00000+00	1.45202+00
9103.68421	3.74330-01	7.02400-02	5.90900-02	2.36300-02	4.25440-01	1.00000+00	1.45202+00
8103.15789	3.74330-01	7.02400-02	5.90900-02	2.36300-02	4.25440-01	1.00000+00	1.45202+00
7102.63158	3.74330-01	7.02400-02	5.90900-02	2.36300-02	4.25440-01	1.00000+00	1.45202+00
6102.10526	3.74330-01	7.02400-02	5.90900-02	2.36300-02	4.25440-01	1.00000+00	1.45202+00
5101.57895	3.74330-01	7.02400-02	5.90900-02	2.36300-02	4.25440-01	1.00000+00	1.45202+00
4101.05263	3.74330-01	7.02400-02	5.90900-02	2.36300-02	4.25440-01	1.00000+00	1.45202+00
3100.52632	3.74330-01	7.02400-02	5.90900-02	2.36300-02	4.25440-01	1.00000+00	1.45202+00
2100.00000	3.74330-01	7.02400-02	5.90900-02	2.36300-02	4.25440-01	1.00000+00	1.45202+00

REFERENCES

1. Moretti, G., B. Grossman and F. Marconi, Jr., "A Complete Numerical Technique for the Calculation of Three-Dimensional Inviscid Supersonic Flows," AIAA Paper No. 72-192, January 1972.
2. Williams, F. A., Combustion Theory, Addison-Wesley Publishing Company, Inc., Reading, Mass., 1965.
3. Moretti, G., "A New Technique for the Numerical Analysis of Non-Equilibrium Flows," AIAA J., Vol. 3, No. 2, February 1965.
4. Stull, D. R., and H. Prophet et al., "JANAF Thermochemical Tables," Second Edition NSRDS-MBS 37, U.S. Department of Commerce, National Bureau of Standards, Washington, D.C., June 1971.

1. Report No. NASA CR-3121	2. Government Accession No.	3. Recipient's Catalog No.		
4. Title and Subtitle Incorporation of Coupled Nonequilibrium Chemistry Into a Two-Dimensional Nozzle Code (SEAGULL)		5. Report Date April 1979		
7. Author(s) Alan W. Ratliff		6. Performing Organization Code		
9. Performing Organization Name and Address Lockheed Missiles & Space Company, Inc. Huntsville Research & Engineering Center 4800 Bradford Blvd. Huntsville, AL		8. Performing Organization Report No.		
12. Sponsoring Agency Name and Address National Aeronautics and Space Administration Washington, D.C. 20546		10. Work Unit No.		
15. Supplementary Notes Langley Technical Monitor: Manuel D. Salas Final Report		11. Contract or Grant No. NAS1-14754		
16. Abstract A two-dimensional multiple shock nozzle code (SEAGULL) has been extended to include the effects of finite rate chemistry. The basic code that treats multiple shocks and contact surfaces was fully coupled with a generalized finite rate chemistry and vibrational energy exchange package. The modified code retains all of the original SEAGULL features plus the capability to treat chemical and vibrational nonequilibrium reactions. Any chemical and/or vibrational energy exchange mechanism can be handled as long as thermodynamic data and rate constants are available for all participating species.				13. Type of Report and Period Covered Contractor Report
17. Key Words (Suggested by Author(s)) Nozzle Flow Finite Rate Chemistry Supersonic Shock Waves		18. Distribution Statement Unclassified - Unlimited		
				Subject Category 34
19. Security Classif. (of this report) Unclassified	20. Security Classif. (of this page) Unclassified	21. No. of Pages 55	22. Price* \$5.25	

* For sale by the National Technical Information Service, Springfield, Virginia 22161

NASA-Langley, 1979